August 2020

Seasonal Infilling And Sedimentary Characteristics In Sandy Versus Muddy Coastal Borrow Areas On The Louisiana Continental Shelf, USA

Matthew Barley

SEASONAL INFILLING AND SEDIMENTARY CHARACTERISTICS IN SANDY VERSUS MUDDY COASTAL BORROW AREAS ON THE LOUISIANA CONTINENTAL SHELF, USA

A Thesis

Submitted to the Graduate Faculty of the
Louisiana State University and
Agricultural and Mechanical College
in partial fulfillment of the
requirements for the degree of
Master of Science

in

The Department of Geology and Geophysics

by
Matthew Trent Barley
B.S., Indiana State University, 2018
December 2020

Acknowledgements

First, I would like to thank Dr. Carol Wilson for her guidance, encouragement, and positivity. Second, I would like to thank Dr. Kehui Xu and Dr. Samuel J. Bentley for their invaluable guidance and feedback given to me during this project. Third, I would like to thank all the PIs on the BOEM SSBA and BBB projects for their critiques on how to improve my project and helping me to think from different viewpoints about my own interpretations. Further, I would like to especially thank Dr. Chunyan Li, Dr. Nan Walker and Haoran Liu for providing additional data processing and assistance.

A special thanks to the invaluable help of staff from LSU Coastal Studies Institute's Field Support Group. Without your assistance, this project would not have been possible!

Finally, thank you to my friends and family. Without your constant support, none of this would have been possible. A special thank you to my Mother and Father, who always encouraged me to chase my dreams and helped shape me into the man I am today.

Funding for this study was provided by the U.S. Department of the Interior, Bureau of Ocean Energy Management, Coastal Marine Institute, Washington DC, under Cooperative Agreement Number M17AC00019. Additional funding was provided through the PADI foundation to complete summer 2019 lab work.

Table of Contents

Abstract

Offshore sand deposits on the Louisiana Continental Shelf, such as inner shelf shoals and buried paleo-river channels, can be excavated to restore beaches and barrier islands that are rapidly deteriorating due to subsidence, sea-level rise and deficits in coastal sediment supply. Presented here is grain size, x-radiograph, and Beryllium-7 (^{7}Be) derived sedimentation rates from multicores (~ 50 cm depth) retrieved from borrow areas (BAs) in contrasting depositional settings, all of which have implications for management of water quality, seafloor sedimentology, and biogeochemistry in proximal areas. Multicores were retrieved in fall 2018 at Caminada BA — a sandy energetic site 25 km offshore of central Louisiana excavated from 2013 to 2016 — and in fall and spring 2019 at Sandy Point BA — a muddy site located 20 km west of Southwest Pass of the modern Mississippi River excavated in 2012.

Results at Caminada for fall 2018 reveal 2 – 6 cm (0.02 – 0.04 cm day^{-1}) of ^{7}Be-laden sediment deposited, significantly less than the 8 – 16 cm (0.05 – 0.15 cm day^{-1}) reported for spring 2018, indicating substantial seasonal variability. There was little difference in median grain size of cores between the two seasons within Caminada BA (12 – 45 μm or 4.5 – 6.5 Φ), with multiple layers of coarser silts seen within x-radiographs. Results at Sandy Point for fall 2019 reveal 2 – 6 cm (0.02 – 0.03 cm day^{-1}) of ^{7}Be-laden sediment deposited, significantly less than the 14 – 34 cm (0.1 – 0.5 cm day^{-1}) reported for spring 2019, indicating greater seasonal variation compared to Caminada BA. There is little difference in median grain sizes of 6.0 – 8.5 μm (~ 7 Φ) between the two seasons at Sandy Point BA, although cores retrieved in fall 2019 have very few to no coarse silt laminations.

Estimates of volumetric and mass infill for Caminada BA reveal that bathymetric low areas are currently infilling at ~ 78,000 m^{3} yr^{-1}, with a predicted 100% infill time of 60 years.

Sandy Point BA is infilling more rapidly at ~ 235,000 m^3 yr^{-1}, with a predicted infill time of 16 years. Analysis of wind/pressure data in tandem with grain size and ^{7}Be activity reveal that winter storms contribute ~ 66 - 73 % of annual infill at Caminada BA in spring 2018 and ~ 10–20 % at Sandy Point BA in spring 2019. Further, Sandy Point BA cores retrieved in fall 2019 revealed 0.3 – 0.5 m of ^{7}Be-dead sediment with a fining-upward pattern, interpreted as rapid deposition following Hurricane Barry. These results are in contrast with numerical models, as infill rates are slower than predicted for both sandy and muddy settings.

1. Introduction

Louisiana is well known for its vibrant communities and dynamic landscape. Protecting Louisiana's coastal land area is of the upmost importance, due to the fact that its wetlands support 30 percent of the commercial fisheries in the United States, 5 of the Nation's top 20 ports are located in coastal Louisiana, and 20 percent of the Nation's oil and gas is sourced or transported through its wetlands (Twilley, 2007; Costanza et al., 2008; Feagin et al., 2010; NOAA, 2010; Gedan et al., 2011). Currently, coastal Louisiana is under threat due to the combined effects of subsidence, storm-induce erosion, sea-level rise, and anthropogenic stresses (Miner et al., 2009; Syvitski et al., 2009). Over the past century, coastal Louisiana has experienced significant change in land area, amounting to a decrease of 25 percent since 1932 (Couvillion et al., 2016). With coastal land loss becoming an ever-growing threat, maintenance and protection of land area in Louisiana is of the upmost importance.

Coastal headlands and barrier islands (sandy sedimentary environments separated from the mainland) act as the first line of defense from extreme weather events, such as hurricanes, which impact the region approximately every 3 years (Neumann et al., 1993), and more frequent but less intense tropical and winter storm events. Additionally, these coastal features are vital for maintaining estuarine conditions further inland (e.g., Penland et al., 1989; Singh et al., 2010). Currently, Louisiana's barrier islands are rapidly deteriorating due to natural factors such as relative sea-level rise (~ 0.9 cm yr^{-1}; Miner et al., 2009) and erosion due to tropical storm-induced waves and currents and anthropogenic factors, such as a deficit in sediment supply to coastal areas due to river management projects (e.g., damming, maintaining navigation channels, and resource exploration upstream: Flocks et al., 2009; Penland and Ramsey, 1990; Miner et al., 2009; Twilley et al., 2016). As sea-level continues to rise at a substantial rate and tropical storms become more

frequent and intense (e.g., Bender et al., 2010; Knutson et al., 2010; Miner, et al., 2009), the protection provided by barrier islands will become even more important.

The Mississippi and Atchafalaya Rivers annually discharge approximately 400 and 87 megatons of suspended sediment, which is primarily transported in suspension and comprised of 90% mud (finer than 63 µm) and 10% sand (Bentley 2002; Walsh and Nittrouer, 2009). Further, bedload material (~ 90% fine sand; Coleman et al., 1998) transported to the Mississippi and Atchafalaya deltas is deposited nearshore as distributary mouth bars, channel sands, and bay fill. Thus, the sedimentary environment of offshore Louisiana is relatively sand poor (see Appendix Figure F1). To restore deteriorating coastal areas, paleo-sand deposits outside of the active coastal system must be targeted and dredged. In order to prevent further land loss, fine to medium grain-sized sand is sought from offshore borrow areas to replenish deteriorating barrier islands and headlands. Borrow areas (BA hereafter) are defined as offshore locations where sand is dredged for restoration purposes. Despite the utility of using BAs for restoration purposes, it is equally important to understand impacts on water quality and seafloor sedimentology, biogeochemistry, topography, and stability in proximal areas.

Implementing coastal restoration projects relies upon the identification of appropriate sand resources and quantification of sand volumes. Studies by the Louisiana Geological Survey (LGS) and the United States Geological Survey (USGS) identified multiple sand resources on the Louisiana-Texas inner continental shelf in a range of depositional systems including spit platforms, delta sheet sands, ebb- and flood-tidal deltas, distributary mouth bars, distributary-channel fills, and inner-shelf shoals (Kindinger et al., 2001). Of these identified sand resources, distributary-channel fills and inner-shelf shoals have become the most important for coastal restoration projects. Although studies have been conducted on the feasibility of extracting restoration quality

sand from sand resources (Khalil et al., 2007; Kulp et al., 2005) and numerical modeling for post-dredge evolution (Nairn et al., 2005), annual geologic coring studies are needed to better understand sediment transport mechanisms and morphological evolution of BAs post-dredging.

In the past, studies have focused on sediment transport processes and morphological evolution of BAs located in both sandy, energetic environments (e.g., Gonzalez et al., 2010; Nairn et al., 2005; and others) as well as more recently in sluggish, muddy environments (Chaichitehrani et al., 2019; Obelcz et al., 2018; Robichaux et al., 2020; Wang et al., 2018; and others). Xue et al. *in review* utilized coring at a sandy BA and found 4 – 12 cm of fine-grained sediments deposited within low-lying areas at rates of 0.02-0.06 cm d^{-1}. Using similar coring methods, O'Connor (2017) found 12 – 34 cm of fine-grained sediment deposited with a muddy BA at rates of 0.12 – 0.34 cm d^{-1}. This study was conducted to better understand how quickly sediment is transported into BAs, where this sediment is sourced from, and how seasonal weather patterns impact the movement of sediment along the Louisiana coast. The goals of this study are as follows: (1) to identify sediment characteristics and quantify infill rates for two specific BAs located in a muddy- versus sandy- depositional environment, (2) to better understand the impacts of storms (tropical and winter) on BA sedimentation in contrasting depositional settings, and (3) to compare estimated time to infill calculated via coring to earlier numerical modeling and bathymetric surveys within the same study areas.

2. Study Area

The largest paleo-sand deposits on the Louisiana continental shelf are generally reworked transgressive shoals, which formed during the final stages of the delta cycle (Roberts, 1997). Submarine shoals along the central Louisiana coast are the remnants of the Maringouin delta complex that was deposited when sea level in Louisiana was 5 – 8 meters below present-day levels (Penland et al., 1986). Penland and Boyd (1981) postulated that the Maringouin delta complex was reworked by marine processes, first into an erosional headland and barrier island system, ultimately submerging into shallow shoals as sediment supply dwarfed relative sea level rise. Trinity Shoal, Ship Shoal, and St. Bernard Shoal are all presumed submerged barrier shorelines that evolved following this progression (Frazier, 1967; Penland et al., 1986).

While submarine shoals represent the largest paleo-sand deposits on the Louisiana continental shelf, their distance (> 10 km) from the shore makes them expensive options for restoration purposes (Penland et al., 1988; Obelcz et al., 2018). More recently, paleochannels have been targeted as alternative sand resources in closer proximity (< 10 km) to the Louisiana coastline. Paleochannels are remnants of former courses of the Mississippi River produced by earlier phases of deltaic occupation and subsequent abandonment (Frazier, 1967). Upon abandonment, the flow velocity dramatically decreases, allowing for suspended sediments to settle. Thus, sand within paleochannels is covered by muddy overburden (~ 1 – 5 m; Obelcz et al., 2018), which must be removed prior to sand excavation.

This study is part of a large, multidisciplinary project on BA morphology, evolution, and environmental impacts on the Louisiana continental shelf that spans several years. This study was focused on two BAs that were sampled during the study period: Caminada BA and Sandy Point BA, further described below.

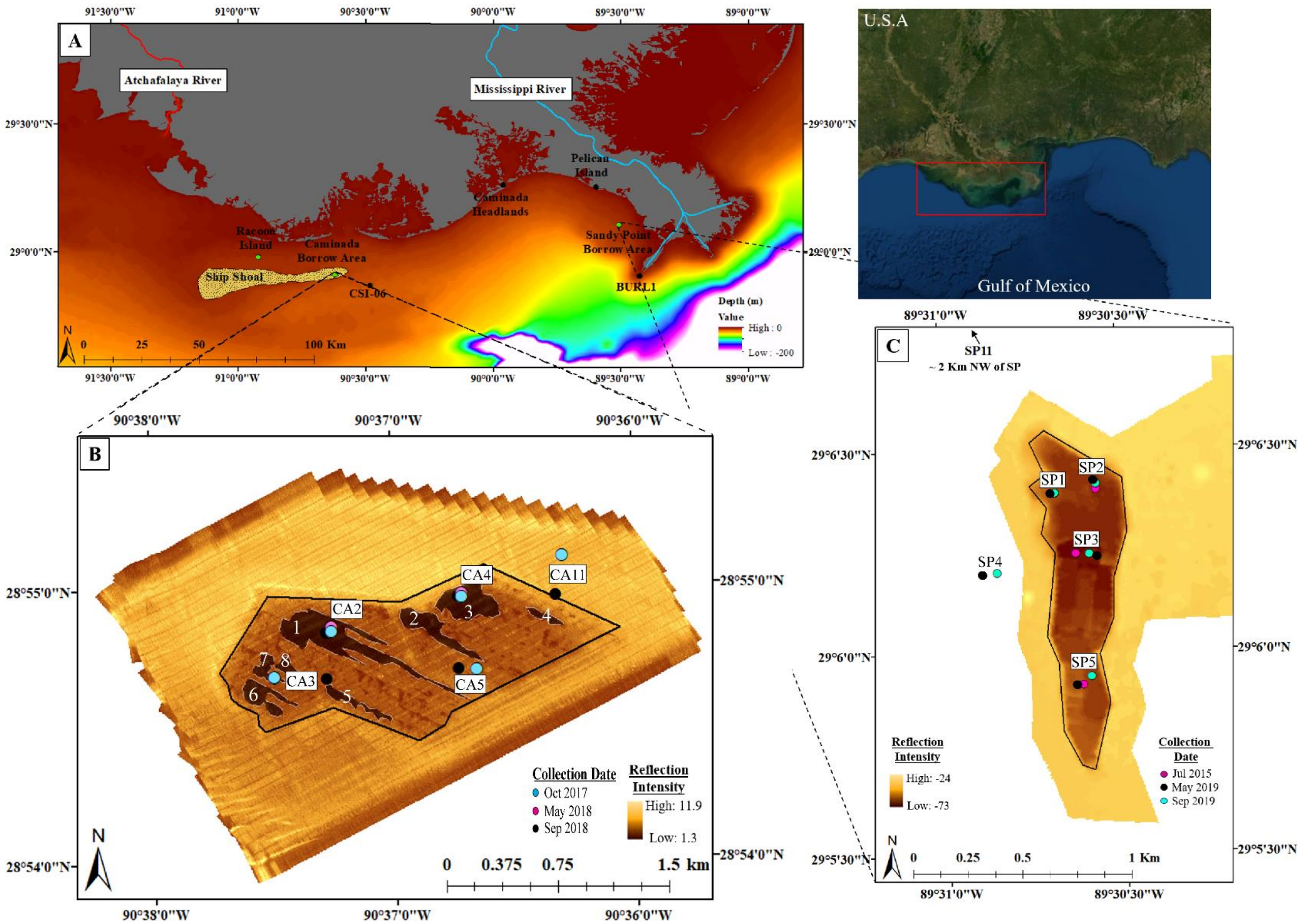

Figure 1. (A) Bathymetric map showing the locations of borrow area study sites, coastal buoys, and restoration sites along the Louisiana coast (Modified from Liu et al., 2019). (B&C) Side scan sonar imagery for Caminada (B) and Sandy Point (C) taken in 2018 and 2012, respectively. The scale represents reflectance values. Areas with low reflectance values (~ 5 for Caminada and -30 for Sandy Point) indicate fine-grained sediment, while high reflectance is indicative of more coarse-grained sediment (Liu et al., 2019; Obelcz et al., 2018). Coring locations are labeled in black lettering, while bathymetric lows are labeled in white for Caminada (B).

1.1. Sandy Borrow Area: Ship Shoal and Caminada BA

Ship Shoal is a sandy inner-shelf shoal located approximately 25 km off the coast of central Louisiana (Figure 1). The shoal is ~ 50 km long by 5 – 12 km wide and located in water depths of 6 – 8 meters, with sediment thickness of 5 – 6 meters aligned parallel to the shoreline (Williams et al., 2011). Ship Shoal is composed almost entirely of sand (volume 1.22 billion m^3) with poorly sorted, very fine sand (2.9 – 3.3 Φ) at the base, coarsening upward into a moderately

sorted, fine sand (2.5 – 2.9 Φ) at the surface (Penland et al., 1986). Caminada BA is located along the 10 m isobath towards the eastern edge of Ship Shoal, excavated in 2013 as part of the Caminada Headland Restoration Project (Fig 1). In total, 8.7 million cubic yards (6.7 million m^3) of sediment were dredged from 6.3 km^2 (1.8 km × 3.5 km) of Caminada BA and transported 50 km to Caminada Headland, restoring over 4.0 km^2 and 22 km of beach from Port Fourchon to Elmer's Island (Coastal Engineering Consultant Inc., 2017). Right after excavation, Caminada BA was ~ 13.7 m below sea level, or ~ 5.7 m below the ambient seafloor depth. Multibeam and seismic surveys performed post-dredging indicate that the seabed is aggrading at a rate of ~ 0.15 m yr^{-1} and infilling approximately 27,500 m^3 yr^{-1} (Liu et al., 2019).

1.2. Muddy Borrow Area: Sandy Point

Sandy Point BA is a buried paleochannel deposit located approximately 20 km north of Southwest Pass of the Mississippi River delta excavated in 2012 for the restoration of Pelican Island, a barrier island located along the Barataria Bay coastline. In total, ~ 3.7 million m^3 of sand was excavated, and the muddy overburden associated with this mud-capped dredge pit was deposited 1.5 km to the east of the BA (Sonders et al., 2014). The maximum pit depth post-dredging was approximately 20 meters below sea level, ~ 11 meters below the ambient seafloor depth. Recent studies estimate that Sandy Point BA is aggrading ~ 0.54 m yr^{-1}, infilling ~ 200,000 m^3 yr^{-1} with a projected total infill time of ~ 15 years (O'Connor, 2017; Obelcz et al., 2018).

3. Methodology

3.1. Geotechnical Field Data Acquisition

Coring field work was conducted on LSU Coastal Studies Institute's *R/V Coastal Profiler* in fall 2018 and spring 2019, and on Louisiana Marine Consortium's *R/V Acadiana* in fall 2019. A total of five sites were sampled at Caminada BA in September 2018 (see Table 1) using an Ocean Instruments MC400 multicorer, which extracts sediment cores to ~ 0.5 m below the sediment-water interface. This method was ideal for this study as it collects four replicate cores per site. Subsequently, a total of 6 sites were sampled at Sandy Point BA, first in May and then in September 2019 (Table 1). The coring method at each site within each BA was the same, using two of the replicate cores with the best penetration depth and preservation: one core was extruded into 2 cm sections on deck (sealed in Whirl-Paks ®) and samples were transported to LSU where they were subsampled for grain size and radiochemical analysis, weighed for water content, and refrigerated (see subsequent sections). The second core was sampled for x-radiography using a Plexiglas x-ray tray (dimensions ~ 60 cm x 8 cm x 2 cm) carefully inserted into the core to preserve sedimentary structures. X-ray samples were also returned to the lab at LSU and refrigerated for processing. This methodology has been successfully used in previous BA studies on the Louisiana continental shelf (see Obelcz et al., 2016; O'Connor, 2017).

Table 1. Core information collected during field cruises

Core Location	Date Collected	Latitude (Degree)	Longitude (Degree)	Length (cm)	Core Substrate
CA2	9/18/2018	28.9139	-90.6214	53	Mud
CA3	9/18/2018	28.9111	-90.6214	27	Mixed
CA4	9/18/2018	28.9161	-90.6123	50	Mud
CA5	9/18/2018	28.9117	-90.6123	12	Mixed
CA11	9/18/2018	28.9161	-90.6055	8	Sand
SP1	5/15/2019	29.1065	-89.5116	54	Mud
SP2	5/15/2019	29.1070	-89.5096	50	Mud
SP3	5/15/2019	29.1039	-89.5095	56	Mud
SP4	5/15/2019	29.1032	-89.5149	16	Mixed
SP5	5/15/2019	29.1032	-89.5105	54	Mud
SP11	5/15/2019	29.1053	-89.5233	32	Mixed
SP1	9/8/2019	29.1065	-89.5114	44	Mud
SP2	9/8/2019	29.1069	-89.5094	36	Mud
SP3	9/8/2019	29.1040	-89.5099	52	Mud
SP4	9/8/2019	29.1033	-89.5142	14	Mixed
SP5	9/8/2019	29.0989	-89.5142	42	Mud
SP11	9/8/2019	29.1308	-89.5202	30	Mixed

SP = Sandy Point, CA = Caminada. Refer to Fig. 1 for core locations

3.2. Radiochemical Analysis of ^{7}Be – Calculation of Short-term Sedimentation

Beryllium-7 (^{7}Be, $t^{1/2}$ = 53.3 days) forms via natural cosmogenic reactions in the atmosphere and is delivered to Earth's surface via dry and wet deposition (Kaste and Baskaran, 2012). Once deposited on the Earth's surface, ^{7}Be forms strong bonds with oxygen atoms, so it adsorbs rapidly onto organic and inorganic solids in terrestrial environments, making it an excellent tracer of fluvial-derived, short term (< 6 months) sediment accumulation in shallow marine environments (Baskaran et al., 1993; Kaste and Baskaran 2013), including the Louisiana continental shelf (Keller et al., 2016; Restreppo et al., 2019).

Upon arrival to LSU, core samples were immediately weighed and subsequently dehydrated at 50 – 60 °C and reweighed to determine water content (%). Samples were then pulverized using a mortar and pestle and packed into petri dishes (50 x 9 mm) to be analyzed for approximately 24 hours on Canberra BEGe, LEGe, and REGe low-background planar gamma detectors. The presence of ^{7}Be was distinguished by a peak at 477 keV. Inventory of ^{7}Be for each core (disintegrations per minute per square centimeter, or dpm cm^{-2}) can be calculated using the equation below from Muhammad et al. (2008):

$$I = \Sigma\rho_s \Delta z(1 - \Phi_i)A_i \qquad (1)$$

where ρ_s is the grain density (g cm^{-3}), $\triangle z$ is thickness of the sample (~ 2 cm), Φ_i is the porosity calculated from water content loss at 50-60° C, and A_i is the activity at depth (disintegrations per minute per gram, or dpm g^{-1}). Calculated ^{7}Be inventories were then compared to annual dry and wet deposition flux from Barataria Bay, LA (5.4 dpm cm^{-2}, Corbett et al., 2004) and from Galveston, TX (14.7 dpm cm^{-2}, Baskaran et al., 1993).

After ^{7}Be activity was assessed, the software SigmaPlot was used to generate depth profiles displaying ^{7}Be activity for each core. Using these profiles, a regression analysis was used to calculate the short-term (~ 5 – 6 month) sedimentation rate using the following equation from Muhammad et al. (2008):

$$A_z = A_0 e^{(-\lambda/S)} \qquad (2)$$

where Az is the activity at depth z, A_0 is the activity extrapolated to the surface (depth = 0), lamda (λ) is the decay constant (0.01307 d^{-1}) and S is the sedimentation rate in cm day^{-1}.

3.3. Grain Size Analysis

Grain size analysis was used to better understand grain size variations within BAs as well as sedimentary patterns within collected cores. Each small (< 2 g) sediment subsample was mixed with 7 mL of sodium metaphosphate ($NaPO_3$, 25 g L^{-1}) in a 50 mL centrifuge tube for deflocculation. Samples were then vortexed until all particles were separated. Next, samples were sieved using an 850 µm sieve into a 20 mL glass test tube, which was subsequently filled up to 90% with $NaPO_3$. Samples were then centrifuged for ~ 1 hour at 30 – 45 rpm until the supernatant was completely separated.

Once the supernatant was discarded, 3 mL of $NaPO_3$ and 5 – 7 mL of hydrogen peroxide (H_2O_2) was added to dissolve organic material. Samples were then submerged in a hot bath, in which temperature was incrementally increased from 50°C to 70°C over a time period of ~ 1 hour, then reduced to 50°C for 24 hours. After 24 hours, the supernatant was removed, and the sediment was transferred to a 50 mL centrifuge tube, 40 mL of $NaPO_3$ was added and the sample vortexed. Samples were analyzed using a Beckman-Coulter LS13320 Aqueous Liquid Module (ALM), and SigmaPlot was used to generate volume-frequency contour plots for distribution of grain size in microns for all samples from all cores. The software Strater 4 was used to make stratigraphic columns that correlate with grain size volume-frequency plots for each multicore.

3.4. X-Radiographs

Cores were imaged using a Thales Flashscan 35 digital X-ray detector illuminated by Medison Acoma portable X-ray. These X-radiographs were then digitized to visually analyze the sedimentary structures within each core using the software ImageJ. Brightness and contrast of images was adjusted for clarity. For all cores >30 cm in length, two digitized x-radiographs were imaged and stitched together to visualize the core in its entirety.

4. Results

4.1. Radioisotope ^{7}Be

Multicores collected at Caminada and Sandy Point BAs showed considerable variability in both ^{7}Be activity and depth of penetration. A summary of results is given in Table 2. For Caminada multicores 2, 4 and 5 (i.e., the three cores within the BA that had ^{7}Be activity), ^{7}Be is present from the surface to depths of 2 – 6 cm. The peak activity for all three cores occurred closest to the sediment-water interface (~ 0 – 2 cm) with values of 11.24 ± 0.63, 12.9 ± 0.59 and 5.3 ± 0.39 dpm g^{-1} for Sites 2, 4 and 5, respectively, and activity showed an exponential decrease with depth (Fig 2). Calculated ^{7}Be inventory was highest at Site 5 and lowest at Site 2 with respective values of 2.30 and 0.60 dpm cm^{-2}. Calculation of ^{7}Be derived sedimentation rate was possible for Sites 2 and 4, yielding values of 0.02 ± 0.01 and 0.04 ± 0.02 cm day^{-1}, respectively, with an average sedimentation rate of 0.03 cm day^{-1}. Site 3 within the pit and Site 11 outside of the pit did not contain detectable ^{7}Be in their samples. Grain size analysis of these coring locations revealed that both sites were sand-rich near the surface (see section 4.3, below).

Sandy Point multicores recovered in May 2019 displayed the largest ^{7}Be inventories and deepest ^{7}Be penetration depths for cores within the BA as compared to September 2019. For Sandy Point multicores 1, 2, 3 and 5 (i.e., the four cores within the BA), ^{7}Be was present from the surface to depths ranging from 14 to 34 cm, and ^{7}Be penetration depth decreased southward in the pit from Site 1 to 3. Peak ^{7}Be activity ranged from 2.89 ± 0.42 dpm g^{-1} to 3.20 ± 0.41 dpm g^{-1}. Despite the aforementioned trend in ^{7}Be penetration depth, calculated ^{7}Be inventory was highest at Site 1 and lowest at Site 3, with values ranging from 0.55 to 3.07 dpm cm^{-2}. Only data from Site 2 showed the typical exponential decreasing trend in ^{7}Be activity with depth (R^2 = 0.7987), and the calculated sedimentation rate was 0.22 cm day^{-1}. Two additional cores were

taken outside of the Sandy Point BA at Sites 4 and 11. No ^{7}Be activity occurred at depth for Site 4, however, Site 11 had activity to a depth of approximately 5 cm (Fig. 2). The highest ^{7}Be activity and total inventory at Site 11 was 1.98 ± 0.30 dpm g^{-1} and 0.48 dpm cm^{-2}, respectively. Additionally, a sedimentation rate of 0.06 cm day^{-1} was calculated for this site, however, a high uncertainty of ± 0.09 cm day^{-1} was associated with this sedimentation rate. These data reveals that sedimentation within Sandy Point BA is occurring approximately 3 times faster than in areas immediately outside.

For Sandy Point multicores recovered in September 2019, results were expected to be like cores recovered in May 2019 due to similar fluvial discharge conditions (Table 2), however this was not the case. At Sites 1, 2, 3, and 5, the ^{7}Be penetration depth ranged from 2 – 6 cm (Table 2). ^{7}Be activity was highest near the sediment-water interface, with values ranging from 1.47 ± 0.41 dpm g^{-1} to 5.92 ± 0.71 dpm g^{-1} (shown in Fig 2). In contrast to May 2019 cores, ^{7}Be inventory was much lower, with the greatest value at Site 5 (0.52 dpm cm^{-2}). Sedimentation rates could only be calculated for Sites 1 and 5, which ranged from 0.017 ± 0.001 and 0.026 ± 0.01 cm day^{-1}, with an average sedimentation rate of 0.022 cm day^{-1} (Table 2). Outside the pit, Site 11 was the only location that had ^{7}Be present at depth (~ 6 cm). The peak ^{7}Be activity was 2.42 ± 0.35 dpm g^{-1} at 4 cm depth, but the total ^{7}Be inventory at this site was very low (0.32 dpm cm^{-2}). The calculated sedimentation rate for Site 11 was 0.068 cm day^{-1}, however, a high error of ± 0.015 cm day^{-1} was associated with this sedimentation rate (Table 2).

Table 2. ^{7}Be penetration, inventory, calculated sedimentation rate and fluvial discharge average over 6 month prior to sampling for the Mississippi (MR) and Atchafalaya (AR) rivers

Retrieval Date	Core Location	Depth of ^{7}Be Penetration (cm)	^{7}Be Inventory (dpm cm^{-2})	Sedimentation Rate (cm day^{-1})	R^2	MR Discharge (m^3 s^{-1})	AR Discharge (m^3 s^{-1})	Core Data Source
Oct-17	CA2	12	3.67	0.06	0.6813	18,931	8,197	Xue et al. (*in review*)
	CA3	8	2.13	0.06	0.7853			
	CA4	4	0.61	0.02	0.019			
	CA5	--	--	--				
	CA11	--	--	--				
May-18	CA2	14	2.61	0.15	0.6860	20,358	8,921	Xue et al. (*in review*)
	CA3	8	2.60	0.05	0.9112			
	CA4	16	2.85	> 0.08	--			
	CA5	--	--	--	--			
	CA11	--	--	--	--			
Sep-18	CA2	4	0.60	0.02 ± 0.01	0.9840	18,228	7,876	This Study
	CA3	--	--	--	--			
	CA4	4	1.24	0.04 ± 0.02	0.7914			
	CA5	2	--	--	--			
	CA11	--	--	--	--			
Jul-15	SP1	28	--	0.26	0.57	20,232	8,958	O'Connor (2017)
	SP2	24	--	0.08	0.81			
	SP3	18	--	0.16	0.42			
	SP4	--	--	--	--			
	SP5	14	--	0.08	0.79			
	SP11	--	--	--	--			
May-19	SP1	34	3.07	0.51 ± 0.27	0.2191	30,559	13,263	This Study
	SP2	30	2.43	0.22 ± 0.036	0.7987			
	SP3	14	0.55	0.12 ± 0.076	0.3362			
	SP4	--	--	--	--			
	SP5	28	2.99	0.40 ± 0.018	0.3580			
	SP11	4	0.48	0.06 ± 0.09	0.3888			
Sep-19	SP1	6	0.42	0.017 ± 0.001	0.9954	30,775	13,880	This study
	SP2	2	0.18	--	--			
	SP3	2	0.14	--	--			
	SP4	--	--	--	--			
	SP5	4	0.52	0.026 ± 0.01	0.9422			
	SP11	4	0.35	0.068 ± 0.015	0.2440			

SP = Sandy Point; CA = Caminada; -- = null values; Calculated Sedimentation Rates from this and other Caminada and Sandy Point studies. Average fluvial discharge data downloaded from Rivergauges.com for USGS stations 07295100 (Miss. River, Tarbert Landing, MS) and 07381490 (Atch. River, Simmesport, LA). Refer to Fig. 1 for coring locations

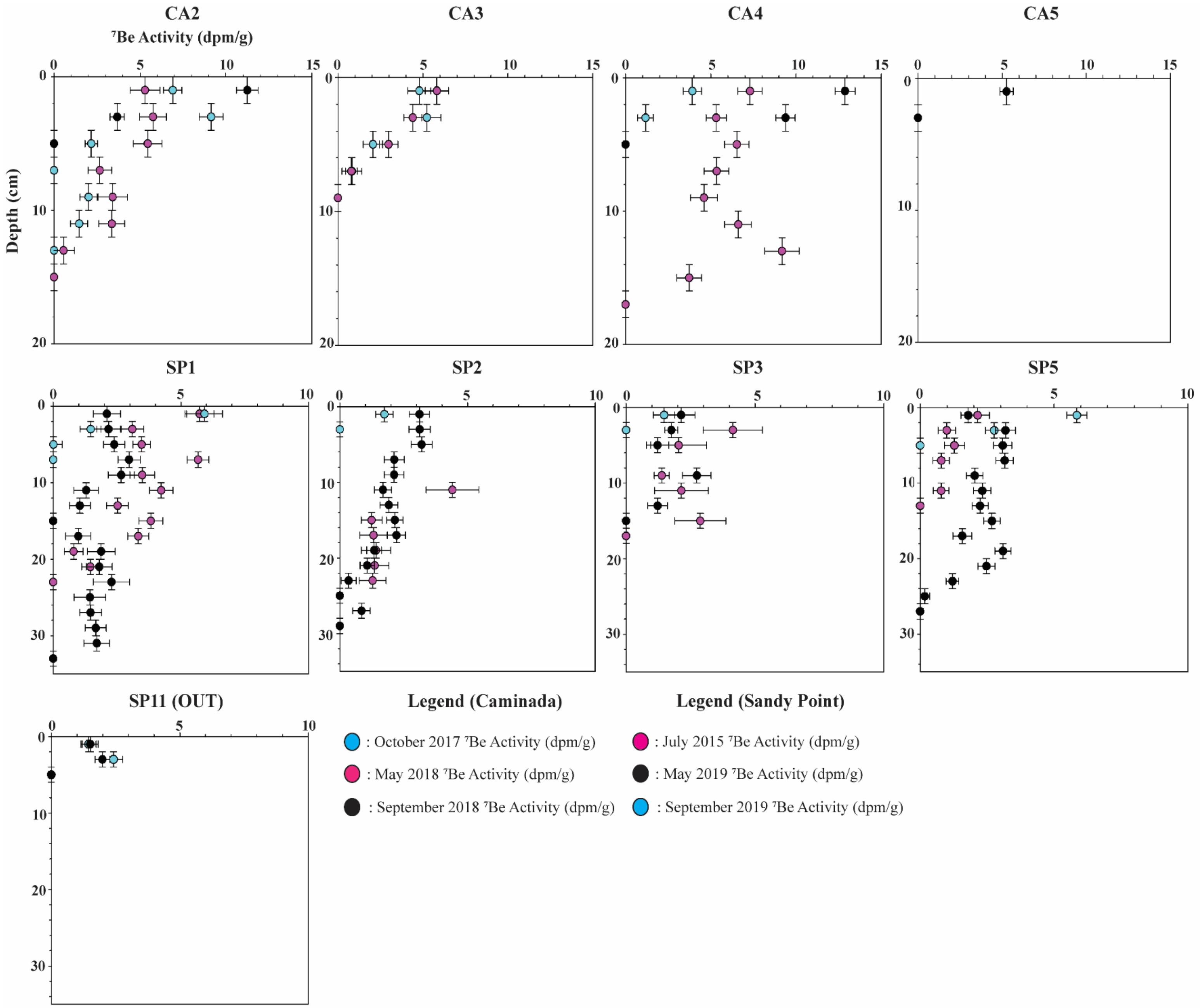

Figure 2. ^{7}Be activity at depth compiled for Caminada (CA) BA and Sandy Point (SP) BA from this study and other recent coring campaigns. For stations CA11 and SP4, no ^{7}Be was present at depth. Data at CA for October 2017 and May 2018 from Xue et al. in review). Data from SP for July 2015 from O'Connor (2017). Regression plots for these data can be found in Appendix A.

4.2. Grain Size

At Caminada BA, recent infill within the dredge pit is dominated by silts, ranging from 30 – 100% by volume. On average, the sediment infill has a median grain size around fine- to coarse-silt, ranging from 12 – 45 µm (4.5 – 6.5 Φ), and contains laminations (< 1 cm) and beds (> 1 cm) of more coarse sediment, median grain size ranging from medium silt to very fine sand, 25 – 125 µm (3 – 5.5 Φ). Clean undisturbed fine sand beds similar to the Shoal Crest facies described by Penland et al. (1986) are found outside of the BA. Figure 3 displays the grain size frequency plots and accompanying stratigraphic profiles for core Sites 2 and 5 within Caminada BA compared to previous results by Xue et al. (*in review*; all core plots and profiles from this study can be found in Appendix B). The results at the two sites are quite consistent: CA Site 2 contained thick packages of fine silt (~ 5 – 20 cm thickness) separated by layers of medium to coarse silt (~ 1 – 10 cm thickness), while Site 5 was coarser than the other sites within Caminada BA, with a median grain size of 103 µm (3.3 Φ). At Site 5, ~ 2 cm of silt was deposited on top of the very fine sand in September compared to May 2018.

Sandy Point BA cores recovered in May 2019 were composed of finer-grained sediment than those collected at Caminada BA. For Sandy Point cores recovered within the BA (i.e., 1 - 3, and 5), 100% of the sediment ranged from clay to silt (< 63 µm or 4 Φ). Beds of medium- to coarse-silt (16 - 63 µm or 4-8 Φ) occurred irregularly and were overlain by massive beds (~ 5 – 25 cm) of clayey silt (e.g., 0 - 20 cm depth in SP1, Fig 3; all core data presented in Appendix A through C). For example, a coarse silt sediment layer can be seen for Site 1 at ~ 45 cm depth (Fig 3). For cores taken outside of the BA (i.e., Sites 4 and 11), median grain size ranged from 10 – 120 µm (3 – 6.5 Φ), with most of the sediment comprised of coarse-silt to fine-sand with a fining-upward pattern (SP4 shown in Fig 3).

Like May 2019, September 2019 cores retrieved from within Sandy Point BA were composed entirely of clay and silt (< 63 µm or 4 Φ), however, grain size patterns differed substantially at many of the sites (see Fig 3 for representative cores). For example, the core retrieved at Site 1 for May 2019 shows multiple medium to coarse silt beds (16 - 63 µm or 4 - 8 Φ) grading into fine-silts and clays (< 16 µm or > 8 Φ). In contrast, in September 2019, only one massive bed (~ 30 cm thickness) of fine silt (< 16 µm) was seen at Site 1. Outside Sandy Point BA, a general fining was observed: at Site 4 the median grain size was within the fine to very fine sand range, averaging 81 µm (~3.5 Φ) in May 2019, however 3 months later in September 2019 the median grain size decreased to an average of medium silt, 20 µm (~ 5.5 Φ; see Fig 3). This change is associated with a thinner sand deposit extracted in September compared to May (12 cm thick to 2 cm thick; see Fig 3); this results in a 25% fining at Site 4. Additionally, Site 11 also fined from May to September, although to a much lesser extent (25 µm to 17 µm).

Table 3. Depth-averaged Grain size median (μm), mean (μm) and lithology for Sep 2018, May 2019 and Sep 2019

Retrieval Date	Core Location	Grain Size Median (μm)	Grain Size Mean (μm)	Predominant Lithology
Sep-18	CA2	12.4	20.0	Fine – Med. Silt
	CA3	42.7	53.4	Coarse Silt
	CA4	16.1	22.3	Medium Silt
	CA5	103.1	100.4	Very Fine Sand
May-19	SP1	8.4	14.2	Fine Silt
	SP2	6.7	11.3	Fine Silt
	SP3	5.9	12.3	Fine Silt
	SP4	80.8	86.4	Very Fine Sand
	SP5	6.7	11.6	Fine Silt
	SP11	24.8	34.6	Coarse Silt
Sep-19	SP1	6.3	12.2	Fine Silt
	SP2	7.9	15.7	Fine Silt
	SP3	8.3	15.1	Fine Silt
	SP4	20.2	29.7	Medium Silt
	SP5	8.0	14.3	Fine Silt
	SP11	17.8	25.1	Medium Silt

SP = Sandy Point, CA = Caminada, Refer to Fig. 1 for core locations

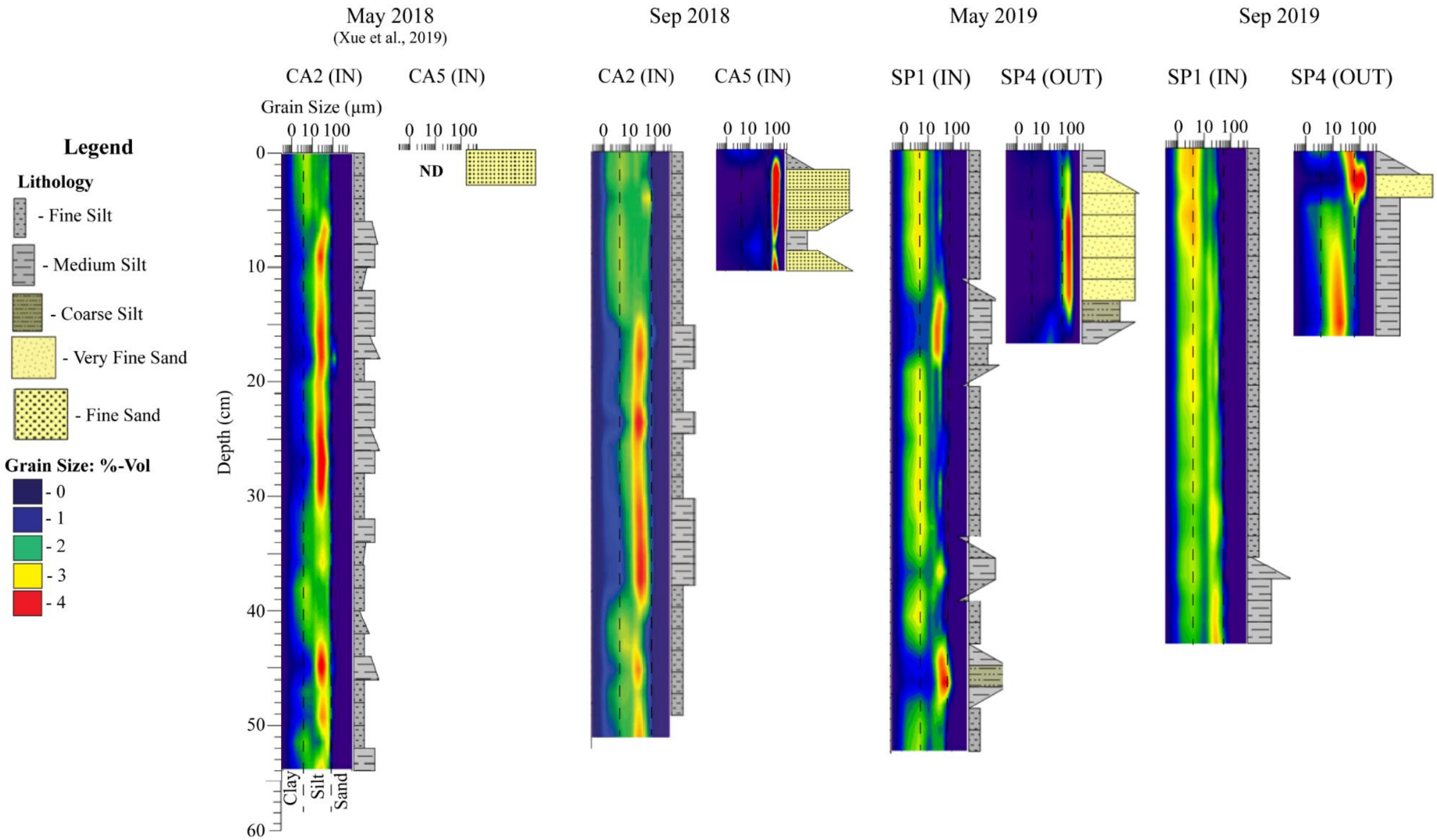

Figure 3. Grain-Size frequency contour plots with stratigraphic profiles for representative multicores collected from Caminada BA (CA) and Sandy Point BA (SP) in May and September 2018, and May and September 2019, respectively. Vertical dashed lines represent the divisions between clay, silt and sand sized sediments. Grain sizes within the BAs is predominately fine silts and clays, with occasional coarse silt and fine sand laminations and beds. ND = Insufficient data to create frequency plot (see Appendix B for all core data from this study)

4.3. X-Radiography

Caminada and Sandy Point BA x-radiographs reveal a variety of sedimentary structures caused by both physical and biogenic depositional processes, which can be seen in Figures 4 and 5. The radiographs for Caminada BA reveal multiple coarse layers of higher density that occur as thin, mm-scale laminations from 1 - 40 cm depths. Additionally, load structures can be seen in several locations (e.g., CA2) caused by coarser, denser sediment being deposited onto fine-grained sediment. Site 3 displays disturbed sediment layers deformed by biogenic (e.g., bioturbation) or physical reworking processes (Fig 4). Sandy Point BA x-radiographs from cores retrieved in May 2019 reveal multiple laminations and beds of coarser sediment. These coarse laminations or beds are gently dipping, which differs from bedding surfaces of coarser sediment at Caminada BA, which were relatively flat (Red Arrow in Fig 5). Overlying coarse sediment layers are massive, structureless beds of dark (fine silt & clay) sediment, typically 10s of centimeters thick. There is a lack of biogenic structures within all cores excluding Site 1 (Fig 5). Sandy Point BA x-radiographs from cores retrieved in September 2019 revealed fewer sediment structures due to malfunctions with the portable x-ray equipment, which lowered the quality of the images seen. There are isolated laminations of coarse sediment present (i.e., SP2 at ~ 38 cm in Fig 5) and mud clasts were also seen at Sites 4 and 5 (SP 4 shown in Fig 5).

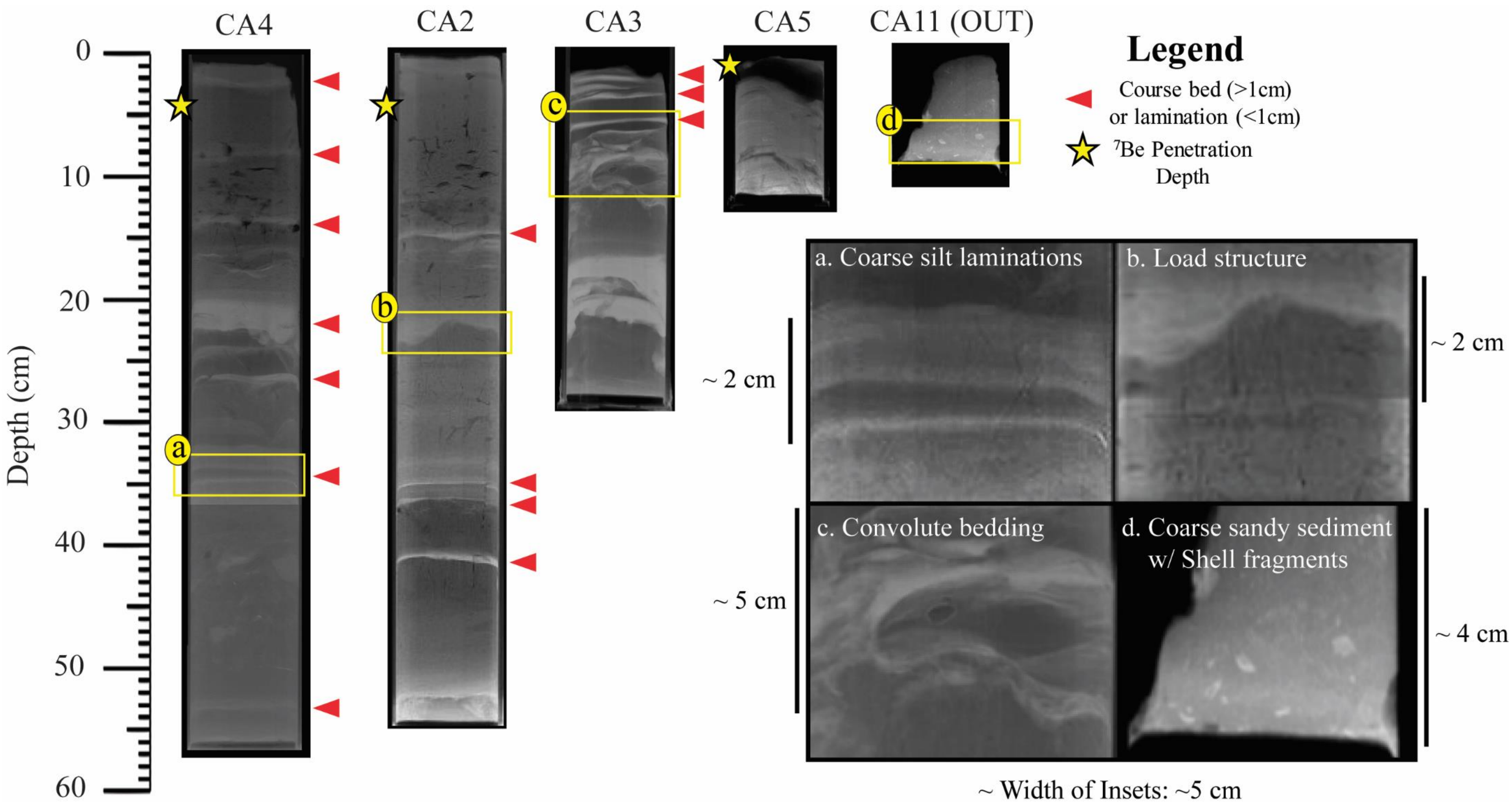

Figure 4. Annotated x-ray images of multicores taken at Caminada BA in September 2018. Light colors represent higher density and larger grain size (i.e., coarse silts & very fine sand) Red arrows represent beds (> 1 cm) and laminations (< 1 cm) of coarse sediment. Areas boxed in yellow are enlarged to highlight sedimentary structures (Unannotated x-rays can be found in Appendix C).

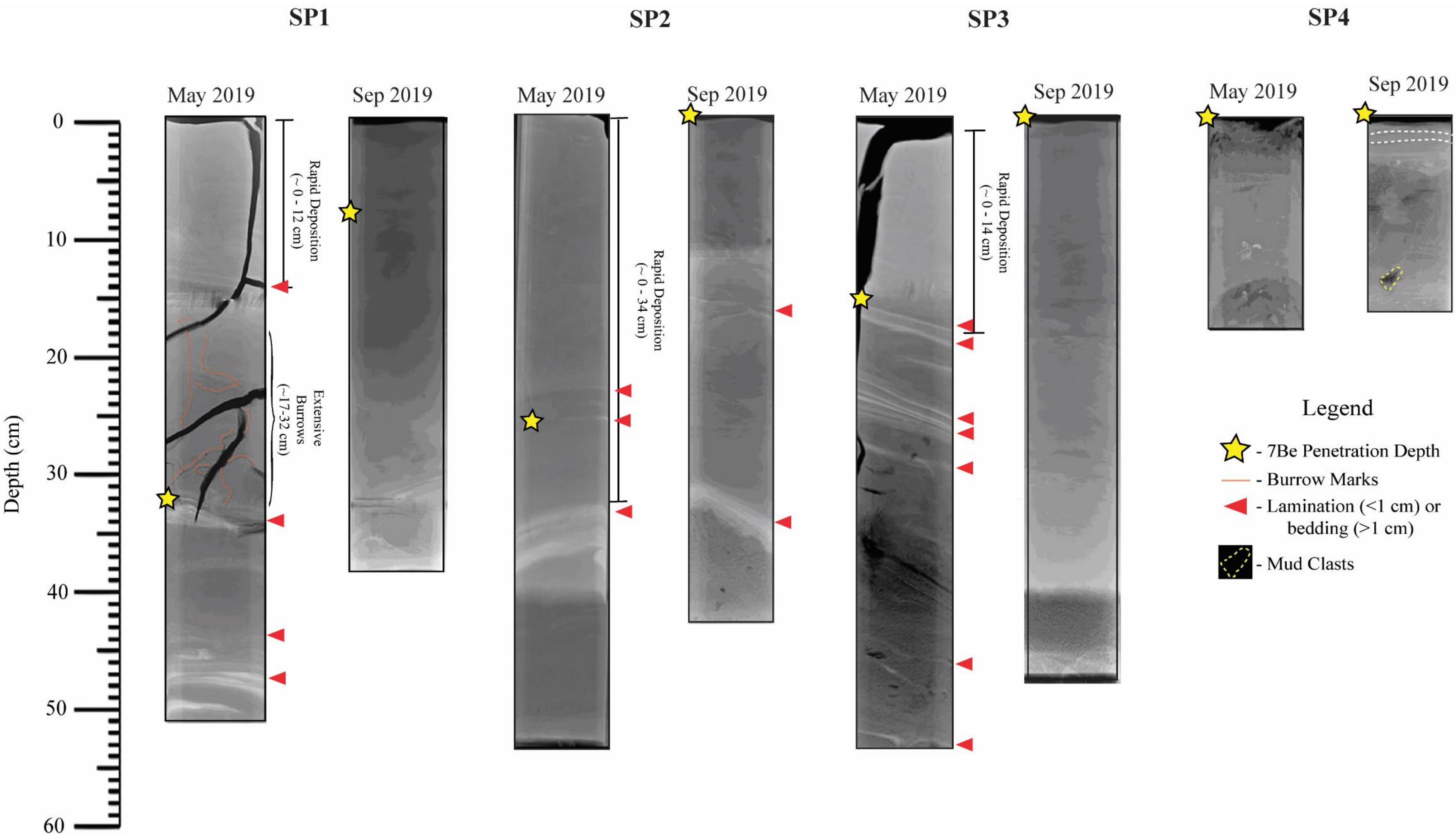

Figure 5. Annotated x-ray images for selected Sandy Point multicores collected in May and September 2019. Dotted white lines represent lamination (< 1 cm) or bedding (> 1 cm) of coarse (white) sediment. Red dotted lines are interpreted as erosional surfaces due to their irregular bedding planes. Red arrows are interpreted as basal portions of rapid sedimentation events. Brown hatched lines represent burrow markings. The yellow star denotes ^{7}Be penetration depth for each core. (Unannotated found in Appendix C)

5. Discussion

5.1. Sedimentation in a Sandy versus Muddy Borrow Area

Potential Sediment Sources to BAs

Possible sediment sources to sandy and muddy Borrow Areas (BA) on the Louisiana continental shelf include fluvial sediment transported by the Mississippi and Atchafalaya Rivers (e.g., Allison et al., 2012; Bentley 2002; Wells and Kemp 1981), resuspended sediments transported from proximal inner shelf and bay areas by storm events (Stone et al., 2009; Walker and Hammack, 2000), or pit wall failure (Nairn et al., 2005; Liu et al., 2019; Obelcz et al., 2018;). Each of these has their own characteristic sedimentological signature, which can be identified using grain size and radiochemical methods, outlined in this section. Once these sediment sources are identified, our study quantifies an estimate of these separate contributions to BA infilling.

Upon entering a delta, sediments transported by a river can be: (1) deposited near the river mouth as part of the delta (subaqueous or subaerial); (2) transported further seaward in a buoyant (hypopycnal) plume; or (3) transported further seaward via a hyperpycnal plume or mass wasting events (Bentley, 2002; Obelcz et al., 2017; Wright, 1985). Fluvial-derived sediments were identified here by the presence of ^{7}Be, as it is an excellent tracer of fluvial-derived, short term (< 6 months) sediment accumulation in shallow marine environments (Baskaran et al., 1993; Kaste and Baskaran 2013), including the Louisiana continental shelf (Keller et al., 2016; Restreppo et al., 2019). Sediment deposited on the continental shelf is typically reworked by oceanic waves, tides, and currents, and in the case of the Mississippi River, can be transported up to 120 km away (Corbett et al., 2004). The use of ^{7}Be as a tracer of fluvial-derived sediment relies on the fact that once deposited, ^{7}Be will naturally decay, leaving

^{7}Be dead fluvial-sediment after ~ 6 months (Baskaran, 2012). Mud percentages from over 50,000 historical grain size samples taken from the Gulf of Mexico reveals that sediment on the Louisiana continental shelf is predominately fine-grained mud (Buczkowski et al., 2006; see Appendix Figure F1). Storm-derived sediment is typically identified by the lack of ^{7}Be and coarser grain size due to higher energy that winnows finer sediment (i.e., Bentley et al., 2002).

Once transported sediments reach a BA, numerical modeling and empirical studies suggest that increased flow depth over BAs reduces sediment carrying capacity, allowing for deposition of fine sediments (Chaichitehrani et al., 2019; Nairn et al., 2005; O'Connor, 2017). Caminada BA is within Ship Shoal, which is a sandy and energetic hydrodynamic setting compared to the surrounding seafloor because it represents a remnant bathymetric high of a drowned delta complex (Stone et al., 2004). Sandy Point, however, is nestled in the crook of the Bird's Foot Delta, which creates a sheltered, sluggish hydrodynamic setting. At Caminada BA, the nearest fluvial sediment sources are quite far: the Mississippi River mouth is ~ 130 km NE and Atchafalaya River mouth is ~ 95 km NW. In contrast, Sandy Point is located ~ 20 km northwest of Southwest Pass on the Mississippi River and thus could receive a greater amount of fluvial sediment exiting the river mouth (Obelcz et al., 2018; O'Connor, 2017; Wang et al., 2018). While our study sites represent two distinct hydrodynamic settings, our results support findings from Xue et al., (*in review*) which indicate that sediment sources to these BAs include fluvial sediment transported by the Mississippi and Atchafalaya Rivers via processes #2 and/or #3 listed above, along with resuspended sediments transported from inner shelf and bay areas by storm events (Stone et al., 2009; Walker and Hammack, 2000).

Lithologic description of vibracores taken from Caminada BA by Xue et al. (*in review*) showed dredging operations left 30 – 80 cm of sandy material with grain sizes consistent with

cores taken on the outside of the pit (2.5 – 3.5 Φ or 100 – 200 μm), which is indicative of ambient Ship Shoal facies described by Penland et al. (1986). Within the pit, this material was topped with ~ 5 – 25 cm of finer grained, ^{7}Be-laden sediment (Xue et al., *in review*). Our study shows that an additional 2 – 6 cm of ^{7}Be-laden mud has been deposited within the pit since the ~ 5 – 25 cm reported by Xue et al. *(in review*), as indicated by radiochemistry, grain size, and x-ray image analysis (Figs 3 & 4). Lithologic descriptions of multicores taken from Sandy Point BA by O'Connor (2017) revealed predominately clay and fine silts (10 – 20 μm), with zones enriched with medium to coarse silts (20 – 30 μm). Our study corroborates that infill at Sandy Point is primarily ^{7}Be-tagged clays and fine silts, with multiple zones enriched with coarser sediment (Figs. 3 and 5).

Sedimentation within BAs can also be sourced from winter and tropical storms. Every year, the northern Gulf of Mexico (nGoM) is impacted by 30 – 40 winter storms (typically called cold fronts), which occur every 3 – 10 days between October and May (Lin et al., 2016; Moeller et al., 1993). Additionally, on average hurricanes impact the nGoM once every 3 years (Neumann et al., 1993), with less intense tropical storms occurring more frequently. The highly energetic waves and currents induced by storm conditions can resuspend coarser sediments such as coarse silts and sands, resulting in erosion and coarse sediment deposition (Corbett et al, 2004; Kobashi et al., 2007; O'Connor, 2017). Additionally, because these sediments are resuspended marine sediments, they could be differentiated from recently deposited fluvial-sediment by the lack of ^{7}Be.

In addition to far-field infill derived from rivers and storm events, infill at Caminada and Sandy Point BA could also be influenced by pit wall failure/readjustment. For example, Obelcz et al., (2018) indicated that pit wall failure was the most significant infill source for Sandy Point

BA immediately after dredging, when pit walls are most unstable. However, repeat bathymetric surveys at Sandy Point BA completed by Obelcz et al. (2018) revealed that pit walls are relatively stable and contributed less than 10% to total pit infill. For Caminada BA, geophysical and geotechnical work indicates that pit wall failure has contributed less than 3 percent to total infill volume (Liu et al., 2019; Xue et al., in review), which is corroborated by results from this study. Additionally, results from our study at Sandy Point revealed no very fine sand-sized particles (~ 80 µm) like that found outside of the pit at Site 4 were found within cores collected in the BA, which would be expected if pit wall failure had contributed to pit infill during our study period. A shortcoming/limitation of this study is that the core locations are all ~ 40 – 320 m from the margins of Sandy Point and Caminada BA, but the consistency of our findings support that pit wall failure does not significantly contribute to infill across the BAs 2 – 6 years after excavation.

Identifying Sediment Source from Type Packages

Previous work by O'Connor (2017) identified three different sediment types within cores recovered from dredge pits (in that case, at Sandy Point, July 2015): The first (Type 1) consisted of high ^{7}Be activity (~ 2 – 5 dpm g^{-1}), clay to medium silt grain size, and low density (i.e., darker) sediments in x-ray core images. Type 2 units consisted of relatively low ^{7}Be activity (0 - 3 dpm g^{-1}), and the sediment was medium-coarse silt, high-density layers (0 - 4 cm thick) evident in x-radiographs. Lastly, Type 3 units had greater concentrations of clay than fine silt compared to Type 1, however the ^{7}Be activity was low (~ 1.5 dpm g^{-1}). Each sediment type was interpreted to represent different seasonal and depositional conditions, with Type 1 sediments inferred as spring deposition (i.e., moderate energy, high discharge, variable ^{7}Be activity, fine to medium silt grain size), Type 2 winter deposition associated with cold fronts (i.e., high energy, low to

zero ^{7}Be activity, medium to coarse silt grain size), and Type 3 summer deposition (i.e., low energy, low discharge, moderate ^{7}Be activity, clay to fine silt grain size; see O'Connor 2017 for details).

Figure 6 shows ^{7}Be activity (dpm g^{-1}) from Caminada and Sandy Point BAs overlain on grain size frequency contour plots, which allowed for identification of sediment types similar to those presented by O'Connor (2017) described above. For Sandy Point cores, our study similarly identifies Type 1, 2 and 3 sediment packages, as well as identify a new (Classified as Type 5) sediment not previously seen within the BA. Type 1 and 2 sediments were similar in ^{7}Be activity, grain size and x-radiographs as those from O'Connor (2017), however our study observed Type 3 sediment with slightly greater ^{7}Be activity compared to O'Connor (2017; ~ 2 – 6 dpm g^{-1} versus ~ 1.5 dpm g^{-1}, respectively). This is likely due to the fact that Type 3 sediment found in this study was in the uppermost ~ 8 cm of cores whereas O'Connor (2017) identified Type 3 sediment from ~ 8 – 20 cm. As ^{7}Be activity decreases with age in a marine environment (e.g., Baskaran, 2012), Type 3 sediments identified herein was more freshly deposited (i.e., had not decayed as much). The newly classified Type 5 sediment was present only in Sandy Point BA cores recovered in fall 2019. Type 5 sediments were ^{7}Be-dead with a distinct bimodal distribution seen in grain size that fines upward from coarse silt to fine silts and clays and appears as low density, massive beds of sediment with brighter basal layers in x-radiographs (exemplified in SP1 & SP2 for September 2019 in Fig 6).

At Caminada BA, our study also observes Type 2 and 3 units in the dredge pit infill, along with a new sedimentary package classified as Type 4. Additionally, re-analysis of core data from Xue et al., (*in review*) led to the identification of Type 1 and 2 sediments in May 2018 cores. For Type 1 sediment, ^{7}Be activity and grain size were similar to that identified for Sandy

Point BA. Type 2 sediment packages, however, were on average thicker at Caminada BA than those identified at Sandy Point BA (~ 8 cm versus ~ 4 cm on average, respectively). Type 3 sediment identified here had higher ^{7}Be activity (~ 4 – 13 dpm g^{-1}) than those identified at Sandy Point in this study and by O'Connor (2017). The newly defined Type 4 sediment consisted of thin (1 - 2 cm) fine sand layers with no ^{7}Be activity (exemplified in CA4 for September 2018 in Fig 6).

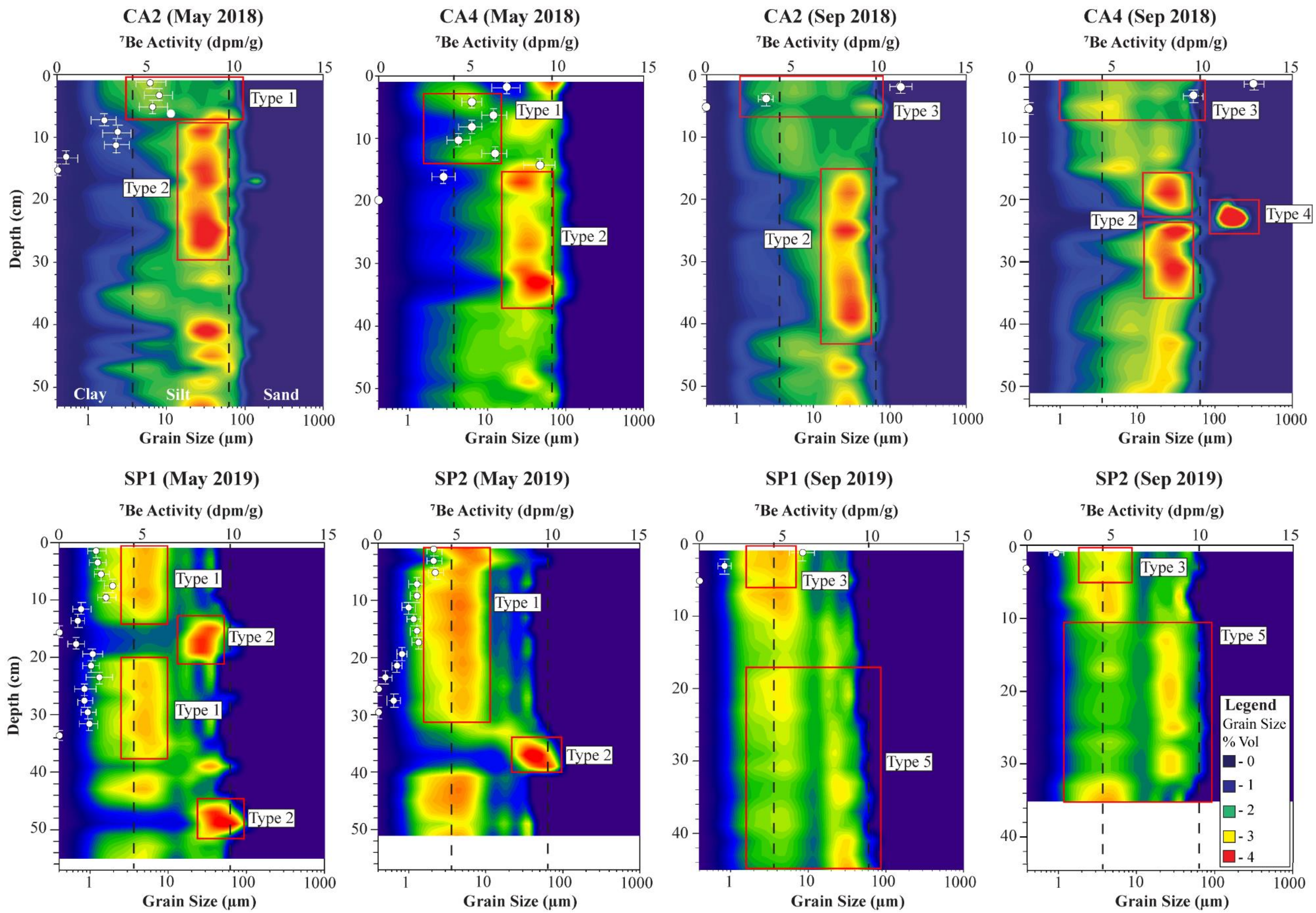

Figure 6. Grain size frequency contour plots with ^{7}Be activity (dpm/g) overlain on top (white circles) for Caminada BA Sites 2 and 4 and Sandy Point BA Sites 1 and 2. Types 1,2 and 3 sediments are similar to those seen by O'Connor (2017) for cores collected at Sandy Point BA in July 2015. Type 4 sediment is a newly identified type seen only at Caminada BA, while Type 5 is only seen at Sandy Point BA (Caminada May 2018 cores taken from Xue et al., in review).

5.2. Temporal comparison of sedimentation in a Sandy and Muddy Borrow Area

Influence of seasonal discharge variation on deposition of Type 1 and 3 sediments

At both Caminada and Sandy Point, Type 1 and 3 sediment were ^{7}Be-laden and fine-grained, indicating that sediment was sourced from proximal rivers, likely hypopycnal plumes due to the distance from the river mouths. One important factor that influences the timing and magnitude of fluvial discharge exiting the Mississippi and Atchafalaya River deltas is the seasonality, with highest and lowest rates occurring in the spring and summer, respectively. To access the relationship between sedimentation and river discharge, daily river discharge data was downloaded from the US Army Corps of Engineers River Gages website (rivergages.com) for the Atchafalaya River at Simmesport and Mississippi River at Tarbert Landing Stations for 2018 through 2019, shown in Figure 7. The areas highlighted in gray represent the ~ 6 month period (~ 200 days, or 4 half-lives due to the ^{7}Be detection limits) prior to the sampling dates, shown as a dotted line for, (A) Caminada in September 2018, (B) Sandy Point in May 2019 and (C) Sandy Point in September 2019. Additionally, Table 2 shows the average discharge for both rivers for the ~ 6-month period prior to sampling dates. Following O'Connor (2017), it is expected that Type 1 sediment will correlate with the rising to peak discharge period, which typically occurs during the months of December to May (Walker et al., 2005; shown in Figure 7). Additionally, Type 3 sediment delivery will be associated with the waning- to low-discharge period, which typically occurs during the months of June to November. The winter storm season predominantly occurs during the months of October to May, and Type 2 sediment deposition is expected to occur during this time (see Fig 7).

Table 4. % of sediment types for cores collected at Caminada and Sandy Point BAs

Borrow Area	Core Site	Date Sampled (mm/yyyy)	% Type 1 & 3	% Type 2	%Type 4	% Type 5
Caminada	CA2	05/2018	27	73	0	0
	CA4	05/2018	33	66	0	0
	CA2	09/2018	66	33	0	0
	CA4	09/2018	80	13	7	0
Sandy Point	SP1	05/2019	80	20	0	0
	SP2	05/2019	88	12	0	0
	SP1	09/2019	17	0	0	83
	SP2	09/2019	21	0	0	79

Percentage sediment type found during different seasons by dividing the thickness of sediment types by the annual infill for selected coring locations (~ 0.3 m yr^{-1} for Caminada and ~ 0.5 m yr^{-1} for Sandy Point). Type 1 and 3 are combined as they represent fluvial-derived material, Type 2 is inferred to be sediment delivered from winter storms, Type 4… (see text for details). Core data for May 2018 taken from Xue et al. (*in review*). See Fig. 1 for Coring Locations

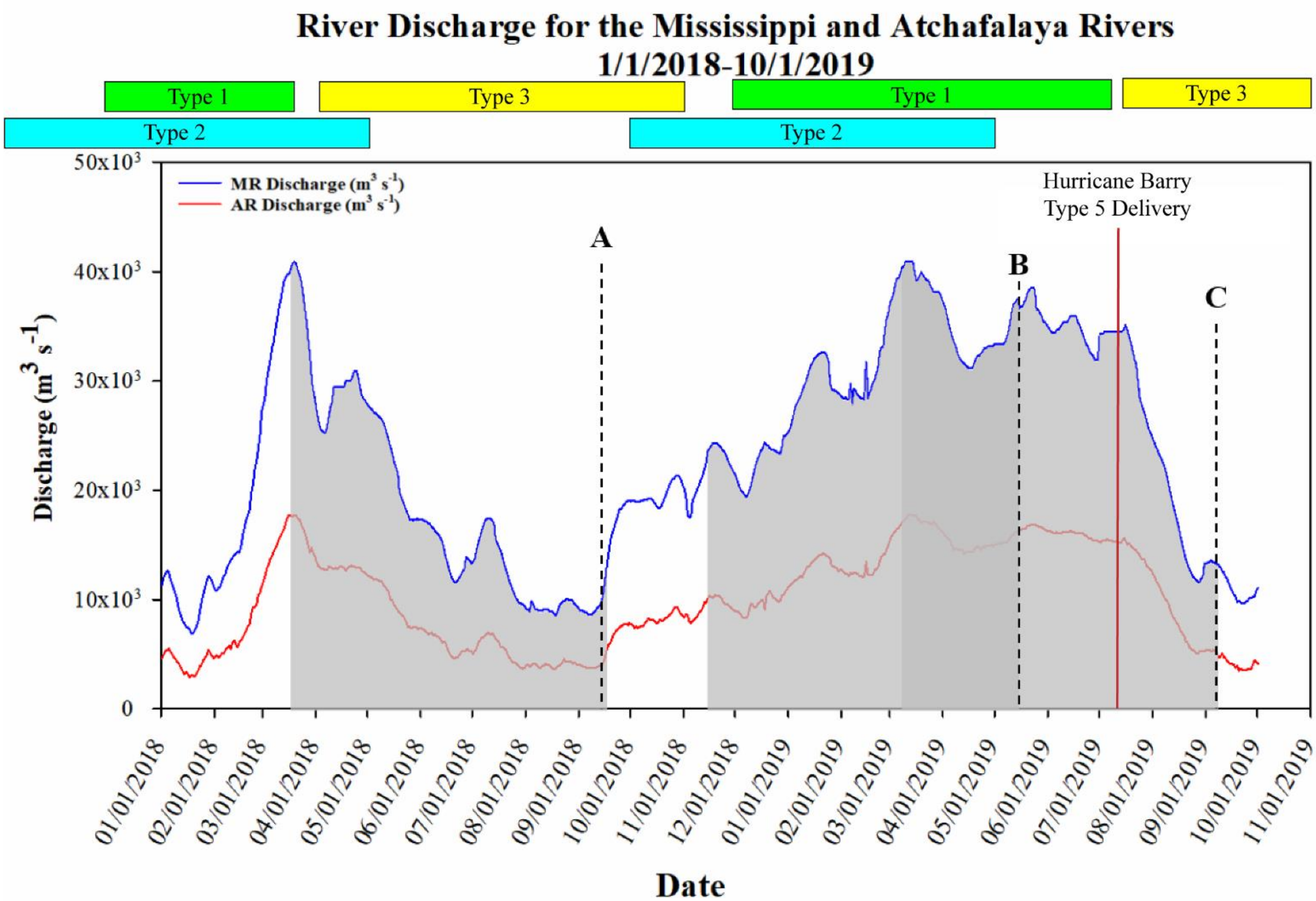

Figure 7. Corps of Engineers Website (rivergauges.com) was collected for the Mississippi River at Talbert Landing, AR and the Atchafalaya River at Simmesport, LA. Shaded areas represent 6 months leading up to coring done for (A) Caminada Borrow Area in September 2018, (B&C) Sandy Point Borrow Area in May and September 2019, respectively. Horizontal bars above the graph represent expected types of sediment delivery during certain river discharge periods. Rapid Type 5 depositions in denoted by a vertical red line at the time of Hurricane Barry.

At Caminada BA, Xue et al. (*in review*) observed an increase in ^{7}Be-derived sedimentation rates from 0.05 cm day^{-1} to 0.10 cm day^{-1} from September 2017 to May 2018, respectively. This increased sedimentation rate coincided with seasonal discharge, specifically an increase in average discharge from 18,931 m^{3} s^{-1} to 20,358 m^{3} s^{-1} for the Mississippi River and 8,197 m^{3} s^{-1} to 8,921 m^{3} s^{-1} for the Atchafalaya River in the period ~ 6 months prior to sampling. In our study, we observed a decrease in the average sedimentation rate from 0.10 cm day^{-1} for spring 2018 to 0.03 cm day^{-1} in fall 2018. Figure 8 displays the significant decrease in ^{7}Be penetration depth, inventory and sedimentation rate from spring to fall 2018, which coincided with a decrease in discharge from 20,358 m^{3} s^{-1} to 18,228 m^{3} s^{-1} for the Mississippi River and 8,921 m^{3} s^{-1} to 7,876 m^{3} s^{-1} for the Atchafalaya River (Table 2). Additionally, Type 1 sediment was present in the uppermost interval (~ 12 cm) of spring 2018 cores from Xue et al. (*in review*) while fall 2018 has Type 3 sediment in the uppermost interval (~ 4 cm; Fig. 6). The sediment type seen in cores corresponds to a shift from Type 1 sediment deposition during the rising to peak discharge period to Type 3 deposition during the waning to low discharge period of the Mississippi and Atchafalaya Rivers illustrated in Figure 7. Analysis of MODIS (Moderate-Resolution Imaging Spectroradiometer) satellite imagery of hypopycnal plumes retrieved from LSU's Earth Scan Laboratory supports the notion that delivery of Type 1 sediment to the pit occurs during high discharge months, while little to no delivery of Type 3 sediment occurs in summer months (see Appendix section E). In addition to fluvial discharge rate, the timing of peak discharge also appears to be correlated to ^{7}Be-derived sedimentation at Caminada (Fig. 7 & Table 2). For example, Xue et al. (*in review*) noted that the increased sedimentation rate from fall 2017 to spring 2018 corresponded with peak river discharge that was ~ 3.5 months prior to coring in September 2017 and ~ 2 months prior to coring in May 2018. Our study also observes

low sedimentation rates for Caminada BA in September 2018 as peak discharge occurred greater than 6 months prior to coring (Fig 7).

At Sandy Point BA, O'Connor (2017) found an averaged sedimentation rate of ~ 0.15 cm day^{-1} for cores collected in summer 2015. Our study reports an averaged sedimentation rate of ~ 0.3 cm day^{-1} for cores collected in spring 2019. Like Caminada BA, the increased sedimentation rate corresponded with increased average discharge from the Mississippi River from 20,232 m^3 s^{-1} to 30,559 m^3 s^{-1} (Fig 7 and Table 2). Atchafalaya river discharge is not reported here because its influence on sedimentation at Sandy Point BA is assumed to be negligible. Figure 8 illustrates this seasonality, with a significant decrease in ^{7}Be penetration depth, inventory and sedimentation rate from spring to fall 2019. For fall 2019, average discharge for the 6 months prior to sampling was similar to spring 2019 (30,559 m^3 s^{-1} versus 30,775 m^3 s^{-1}), however, the Mississippi River exhibited an unusually extended high discharge period during the summer of 2019 (Figure 7). Sampling for September 2019 occurred when the river was in its waning to low discharge period after the passage of Hurricane Barry (Fig 7). As a result, Type 1 sediment is present in spring 2019 cores from 0 – 30 cm depth, while fall 2019 has Type 3 sediment, but only in the uppermost interval (~ 4 cm; Fig. 6). The much larger quantity of Type 1 sediment (~ 30 cm) found at Sandy Point compared to Caminada (~ 10 cm; refer to Figure 6) could be linked to the higher discharge in the ~ 6-month period prior to coring (30,559 m^3 s^{-1} for Sandy Point versus 20,358 m^3 s^{-1} for Caminada), however, proximity to sediment source could also have some control (Obelcz et al., 2018). Analysis of MODIS satellite imagery of hypopycnal plumes reveals greater suspended sediment concentrations over Sandy Point during high discharge months, with decreasing concentrations during waning to low discharge months (See Appendix section E) At Sandy Point BA, Type 1 sediment in cores is correlated to the rising to peak

discharge period, while Type 3 sediment corresponds to the waning to low discharge period of the Mississippi River (Fig. 7).

Results from both study sites are consistent with studies in the Chenier Plain by Rotondo and Bentley (2003), which observed high ^{7}Be inventories (1.2 – 5.4 dpm cm^{-2}) for samples collected in May 2001 and low inventories (< 1.2 dpm cm^{-2}) for October 2002 (See Table 2 for ^{7}Be inventories in this study). Additionally, work done in Fourleague Bay (~ 20 km southeast of the Atchafalaya delta) by Restreppo et al. (2018), which found that ^{7}Be inventories were highest in Spring (e.g., 0.5 – 24 dpm cm^{-2} for March 2016) and lowest in summer and fall (e.g., < 1.4 dpm cm^{-2} for September 2015) is also consistent with our results. On average, ^{7}Be inventories were lower than inventories reported by Rotondo and Bentley (2003) and Restreppo et al. (2018). This is most likely due to mixing of sediment from different sources with different residence times (also seen by O'Connor, 2017 and Xue et al., *in review*), most likely caused by storm events, which is discussed in the following sections.

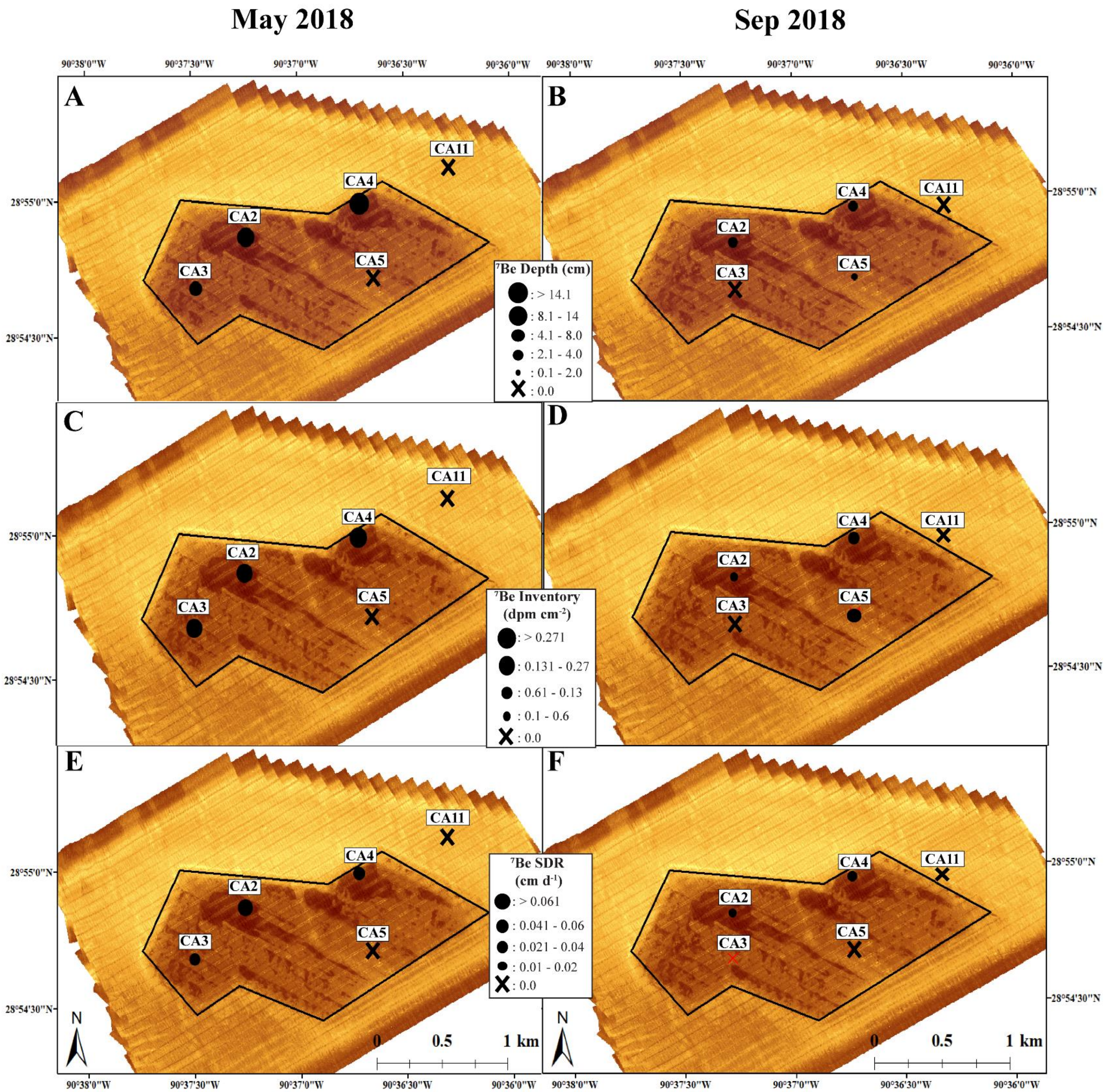

Figure 8. ^{7}Be penetration depths (A&B), inventory (C&D) and sedimentation rate (E&F) plotted in ArcGIS over a sidescan sonar map generated in 2018 by Liu et al. (2019) for Caminada. Darker brown shows muddy, low reflectivity sediment while lighter browns are sandy sediments. Images A, C and E are from May 2018 results from Xue et al. (in review). B, D and F are from September 2018 results from this study

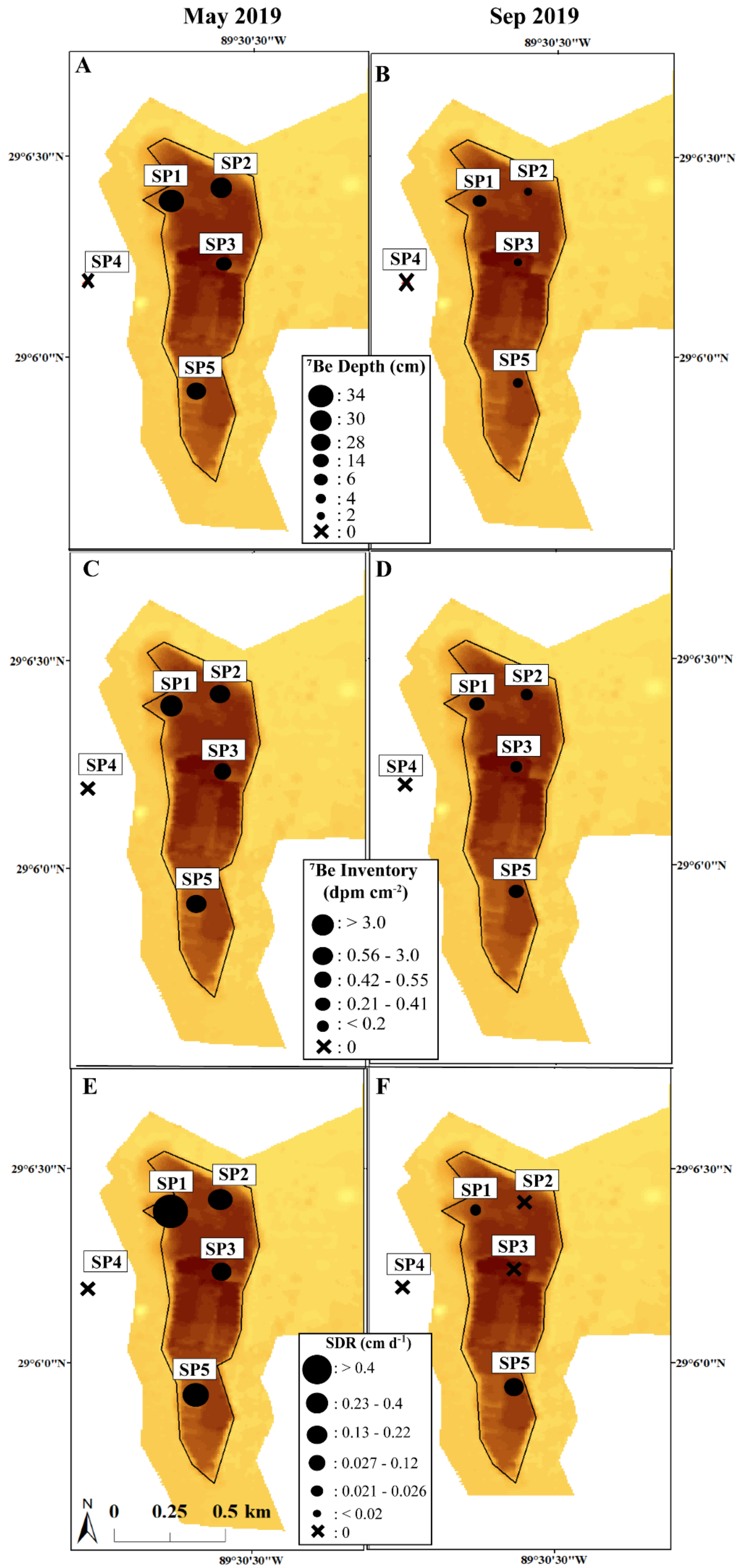
May 2019
Sep 2019
89°30'30"W
29°6'30"N
29°6'0"N
A
B
C
D
E
F
SP1
SP2
SP3
SP4
SP5
^{7}Be Depth (cm)
: 34
: 30
: 28
: 14
: 6
: 4
: 2
: 0
^{7}Be Inventory (dpm cm^{-2})
: > 3.0
: 0.56 - 3.0
: 0.42 - 0.55
: 0.21 - 0.41
: < 0.2
: 0
SDR (cm d^{-1})
: > 0.4
: 0.23 - 0.4
: 0.13 - 0.22
: 0.027 - 0.12
: 0.021 - 0.026
: < 0.02
: 0
N
0
0.25
0.5 km

Figure 9 (Previous page). ^{7}Be penetration depths (A,B), inventory (C,D) and sedimentation rate (E,F) at Sandy Point. A, C and E are from data collected from cores recovered in May 2019, while B, D and F are from September 2019. Basemap is 2012 sidescan sonar data generated by Obelcz et al. (2018) whereby darker brown shows muddy, low reflectivity sediment while lighter browns are sandy sediments.

Deposition of Type 2 sediment following winter storms

Under normal conditions along the Louisiana coast, east winds are predominant, occurring ~ 64% of the year and generating westward wind-driven currents (e.g., Walker and Hammack, 2000). Our study finds that during these quiescent conditions; Type 1 and 3 sediments are deposited within Caminada and Sandy Point BAs (Fig 6). Winter Storms can be identified by a shift in wind direction from the southeast to north, along with a drop in barometric pressure (Stone et al., 2009). During winter storm events, normal westward flow of sediment is disturbed (Walker and Hammack 2000). Further, energetic conditions associated with the passage of cold fronts resuspends coarser, marine sediments (i.e., Type 2 sediment) that are different from that deposited within BAs under quiescent conditions during high discharge months (i.e., Type 1 sediment; Corbett et al., 2004; O'Connor 2017).

To investigate the relationship between the passage of cold fronts and deposition of Type 2 sediment at Sandy Point and Caminada BAs, atmospheric and oceanographic data were collected from coastal buoy stations. For Caminada BA, wind speed and barometric pressure data was retrieved from Louisiana State University's Wave-Current-Surge Information Systems (WAVECIS) CSI-06 meteorological and hydrodynamic monitoring station. For Sandy Point BA, the same data was collected from the National Oceanographic and Atmospheric Administration's (NOAA) coastal buoy BURL1 (See Fig. 1 for buoy locations). This data was then compared to grain size frequency plots, which were converted into time series using average ^{7}Be-derived sedimentation rates for Caminada and Sandy Point coring Sites 2 and 1, respectively. Converting

grain size frequency images to time-series allowed for easy comparison of observed ages of Type 2 sediment deposits to high wind-speed events and drops in barometric pressure, which is indicative of storms. Sites CA2 and SP1 were chosen because they had a calculatable sedimentation rate for each study period. The results of this analysis are shown in Figure 10. For Caminada BA, the calculated timing of Type 2 sediment deposits corresponds to winter storm season in the nGoM (i.e., October to May; Fig 10A-B). At Sandy Point, Type 2 sediment also corresponds to the winter storm season, however, coarse silt layers appear to correspond to particular storm events more distinctly than at Caminada BA (Fig 10C-D). Overall, our findings support conclusions from O'Connor (2017) that winter storms produce Type 2 (Coarse silt) sediment deposits within BAs during high discharge/winter storm season.

Chaichitehrani et al. (2019) used Delft3D model simulations at Sandy Point BA to simulate sediment transport over the pit during a cold front event in November 2014. Their model simulation found that the cold front event halted normal sedimentation at Sandy Point BA and the majority of infill during the event came from seabed resuspension. Further, model estimates of infill at Sandy Point BA from the above study concluded that ~ 16 - 24% of the annual sedimentation is due to cold front events. To investigate the validity of this, model estimates of winter storm deposition was compared to the total thickness of Type 2 sediments (i.e., winter storm deposition) seen within Caminada and Sandy Point BA cores collected in spring 2018 and 2019, respectively. For Caminada, the percentage of Type 2 sediment was calculated by dividing by the annual infill (0.3 m), which was obtained by using high and low infill rates from several studies (Liu et al., 2019; Xue et al., *in review*; this study). At Sandy Point BA, the same method was used, with an annual infill of 0.5 m obtained from high and low infill rates from several studies (Obelcz et al., 2018; O'Connor, 2017; this study). Results from this

analysis are shown for specific coring sites in Table 4. Our results indicate that winter storms deposited ~ 12 – 20% of the annual infill seen within Sandy Point cores collected in May 2019. In comparison, our study estimates that 66 – 73% of annual infill within Caminada BA cores collected in May 2018 by Xue et al (*in review)* was from winter storms. The higher percentage of Type 2 sediment contribution to estimated annual infill at Caminada BA is possibly due to the greater distance from a fluvial sediment source compared to Sandy Point. For example, results from this analysis show Type 1 sediment contributed 80 – 88% of annual infill for spring 2019 cores, compared to only 27 – 34% for Caminada BA cores from spring 2018. Sandy Point BA's closer proximity to a fluvial sediment source provides evidence as to why Type 2 sediment makes up a lower percentage of its annual infill, as it receives greater amounts of fluvial sediment (i.e., Type 1 and 3; ~ 80 %, respectively) during quiescent conditions (Fig. 6 & Table 4). This suggests Caminada BA receives a greater percentage of its total infill during winter storms because of the smaller contribution of fluvial-derived sediment during high discharge, quiescent conditions (Table 4).

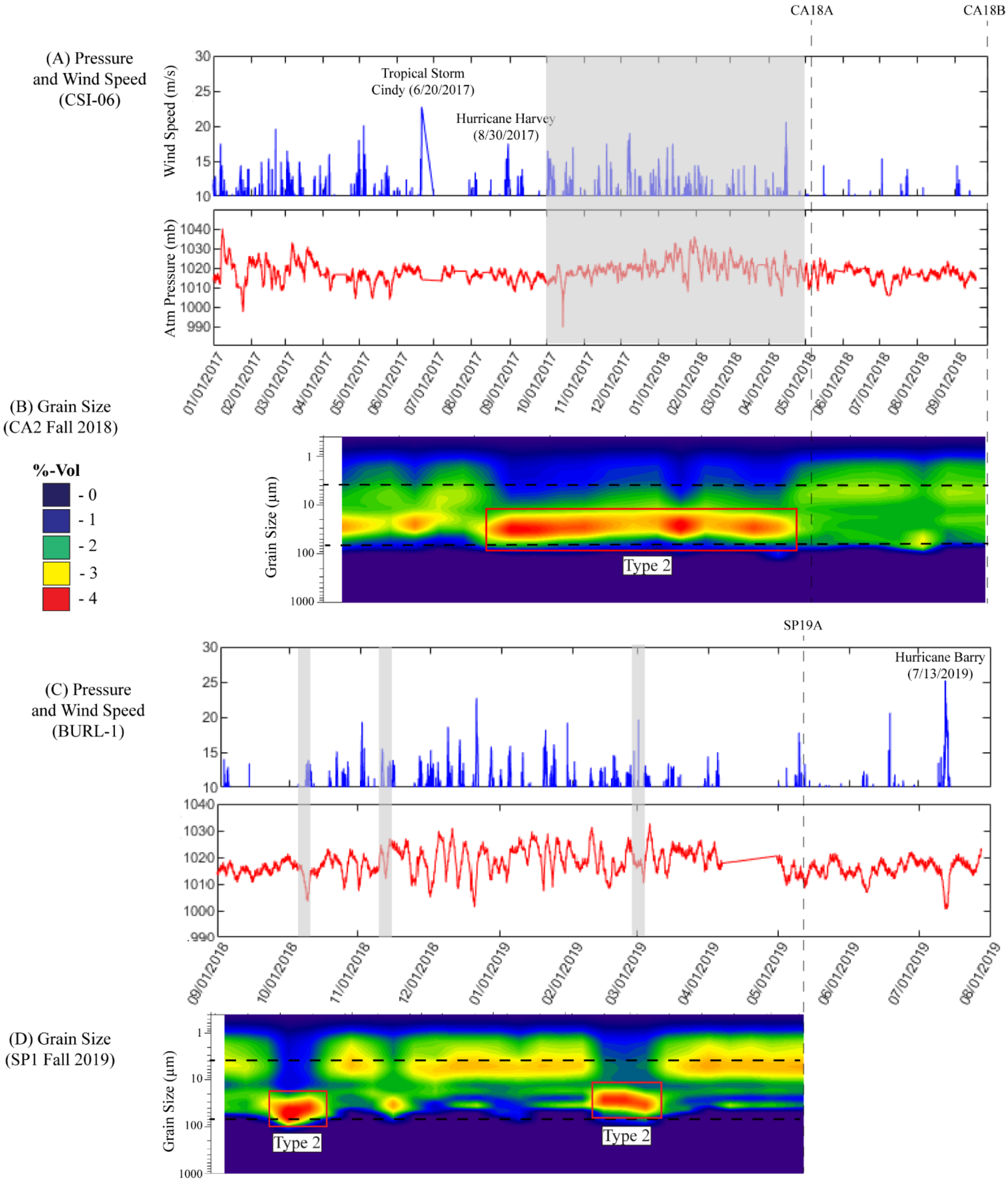

Figure 10. Wind and barometric time series data retrieved from LSU's Coastal Studies Institute buoy number 6 (A: CSI-06) and NOAA coastal buoy BURL-1 (C). Wind speed (in blue) is displayed in meters per second and barometric pressure (in red) is in millibars. Sampling dates for CA18A (Xue et al., in review), CA18B, and SP19A are shown as vertical dotted lines. Areas highlighted in gray represent winter storm season for Caminada (B) and observed timing of storm events (C). (B&D) Grain size frequency contour plots for Caminada Site 2 (B) and Sandy Point Site 1 (D).

Evidence for rapid sedimentation at Sandy Point following Hurricane Barry

In the past, studies have shown that nearshore BAs in Florida capture up to four years of longshore sediment bedload transport volumes following the passage of hurricanes, which generate large waves conducive to pit infilling (Kennedy et al., 2010). However, there is a lack of knowledge on how BAs along Louisiana's continental shelf respond to hurricanes and tropical storms. Previous work has shown that high-energy wave conditions generated by both winter- and tropical storms are conducive to sediment delivery across the Louisiana continental shelf (Bentley et al., 2002; Stone et al., 2004). Further, previous work done at Caminada BA by Xue et al. (*in review*) found that the timing of two 2017 tropical storms correlated well with coarser beds seen in x-radiographs, suggesting storm induced deposition. Compared to 2017, the summer of 2018 was a mild tropical storm season with no major storms, which is confirmed by wind and barometric pressure data (Fig. 10A, above).

The Louisiana coast was not impacted by a hurricane during the summer of 2018, however, Hurricane Barry formed over the nGoM on July 11th, 2019 and made landfall on July 13th, 2019, reaching wind speeds of up to 25 m s^{-1} (Fig. 10C). Sandy Point coring in September 2019 occurred approximately 55 days after Hurricane Barry. Prior to coring, we hypothesized that ^{7}Be penetration depths and sedimentation rate at Sandy Point BA would be similar to May 2019, due to the slight increase in average fluvial discharge (Table 2, above). However, this was not the case, as ^{7}Be penetration, inventory and calculated sedimentation rates were much lower for September 2019 compared to May 2019 (calculated sedimentation rates were 0.22 cm day^{-1} versus 0.02 cm day^{-1} for May and September 2019, respectively).

Keen et al. (2006) found that Hurricane Katrina deposited a storm bed east of landfall on the Louisiana continental shelf with a maximum observed thickness of 0.58 m using sediment

core data. Additionally, studies of multiple hurricane event layers along the Louisiana continental shelf reveal a fining upwards pattern in sediment cores (Allison et al., 2005; Goni et al., 2006; Keen et al., 2005). Numerical modeling using the Regional Ocean Modeling System found that Hurricanes Katrina and Rita were able to erode up to ~ 1.5 m of sediment from the seabed from shear stress generated by storm-induced waves and currents, with the deepest erosional depths occurring east of the hurricane tracks (Xu et al., 2016). Further, estimated sediment flux during these two hurricanes revealed net erosion of sediment in shallow waters and deposition in deeper water. Outside of Sandy Point BA, interpolated mud fraction from the USSEABED reveals that the majority of sediment on the seafloor is mud (finer than 63 µm; Buczkowski et al., 2006; See Appendix Figure F1). Taking the findings of these previous studies into account, we would expect to see resuspension/erosion of sediment outside of Sandy Point BA (i.e., shallow water) and deposition within the pit (i.e., deeper water) following Hurricane Barry. Further, retrieved sediment cores will have a fining-upwards pattern, with the coarsest mud fraction (i.e., coarse silts) at the base of cores.

Following Hurricane Barry, approximately ~ 10 cm of sediment erosion was observed outside of the Sandy Point BA at site 4, inferred by a decrease in sand percentage from 84 % (~12 cm) to 17% (~2 cm) for cores recovered in May and September 2019, respectively. Within the BA, approximately one meter of muddy sediment was deposited, completely burying a tripod deployed by Bales et al. (*in prep)* at the time of the storm. Additional evidence of rapid sediment accumulation at Sandy Point was obtained through analysis of cores within the BA. First, only the uppermost ~ 6 cm of all cores collected within Sandy Point BA contained ^{7}Be, which is inferred to be Type 3 sediment deposited following the passage of Hurricane Barry. Underlying Type 3 sediment is the newly classified Type 5 sediment (see Fig. 6), which was characterized as

^{7}Be-dead with a distinct bimodal distribution seen in grain size that fines upward and appears as low density, massive beds of sediment with brighter basal layers in x-radiographs (Fig. 5). The fining-upwards pattern was seen most clearly at site SP3, exemplified in Figure 11 below. The bimodal distribution seen in Type 5 sediment differs from sediment deposited under quiescent conditions (Type 1 and 3), which only shows a unimodal clay to fine silt grain size. This analysis provides evidence that most sediment within cores collected in September 2019 was sourced from seabed resuspension of older, ^{7}Be dead material that was rapidly deposited in Sandy Point following Hurricane Barry.

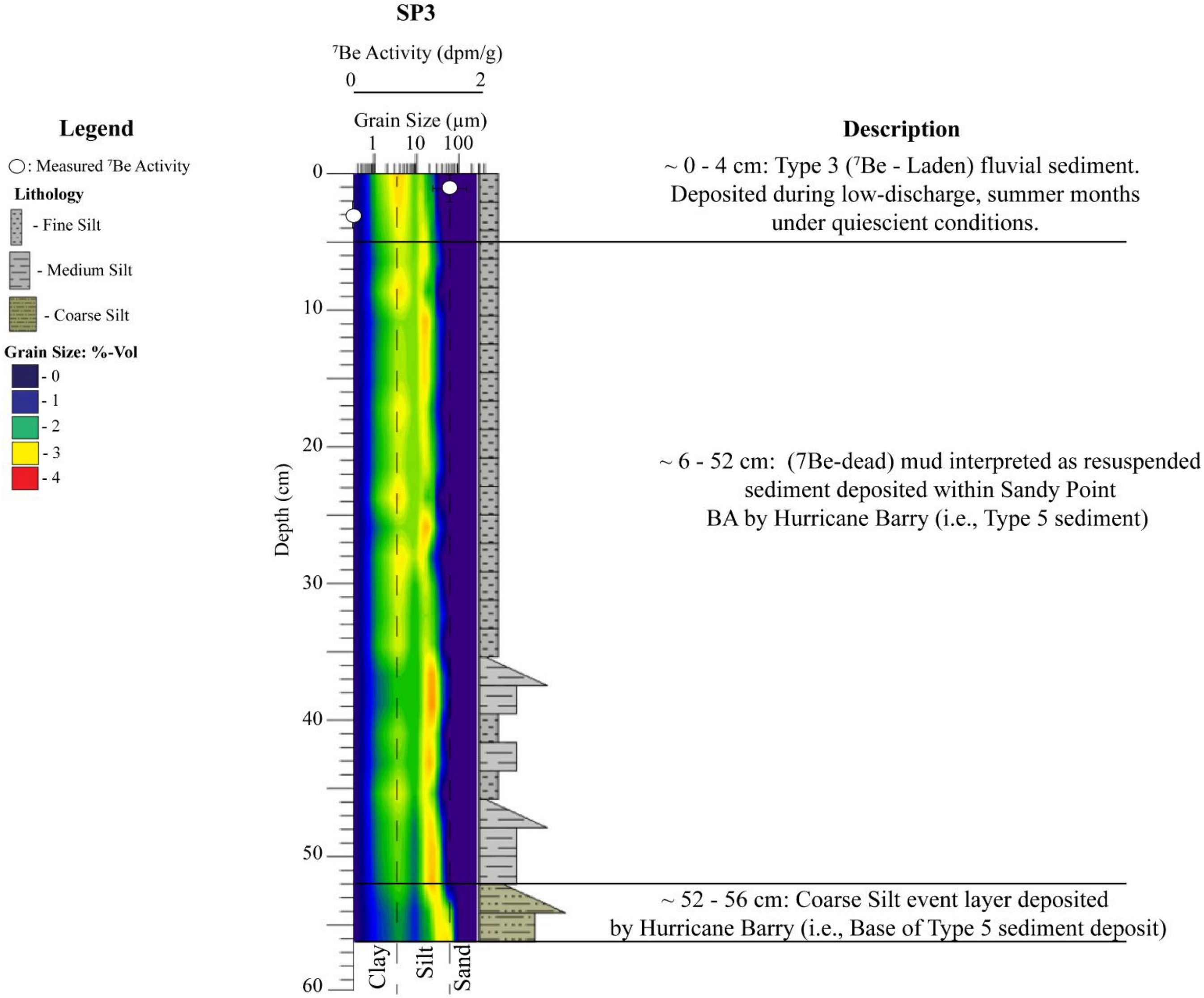

Figure 11. Grain size frequency contour plot with a stratigraphic log showing the median grain size for ~ 2 cm intervals for Sandy Point Site 3 multicore recovered in September 2019. On the right, lithological interpretations are given for the defined core intervals, including Hurricane Barry characterized by bimodal grain size distribution with coarsest mud fractions at the base of the core.

5.3. Volumetric and Mass Accumulation Rate for a Sandy and Muddy Borrow Area

Several studies have attempted to quantify the time to infill BAs in both muddy and sandy depositional settings using numerical modeling and observational data. Nairn et al. (2005), for example, used a 1-D model simulation to estimate infill rate at Sandy Point BA, yielding a time to infill of ~ 10 years, with sediment mainly sourced from suspended sediment plumes. Using the same approach, Nairn et al. (2005) also estimated that BAs in sandy seafloor settings would infill in ~ 5 years, with sediment sourced primarily from bedload transport. Additionally, 1-D modeling was used to study Peveto Channel BA (referred to as Holly Beach dredge pit) post-dredging in 2003. Results of this modeling revealed a lower time to infill of ~ 6 years as compared to other BAs in muddy depositional settings (Nairn et al., 2005; Yu and Nairn, 2011). Later observational studies based on repeat bathymetric surveys completed on Peveto Channel revealed that the pit was completely infilled by 2016, however, no surveys were completed on the BA from 2007 - 2016. Thus, it is likely that Peveto Channel was infilled within 6 – 7 years as suggested by modeling by Nairn et al. (2005). Difference of depth (DoD) analysis at Sandy Point from three post-dredging bathymetric surveys revealed that the BA was infilling at a rate of ~ 0.54 m yr^{-1} (200,000 m^3 yr^{-1}), with a projected time to total infill of 15 years (Obelcz et al., 2018). Similar DoD analysis at Caminada post-dredging revealed that the pit was infilling much more slowly at a rate of ~ 0.15 m yr^{-1}, or 27,380 m^3 yr^{-1} volumetrically (Liu et al., 2019).

While both numerical modeling and bathymetric surveying are useful for identifying overall trends in infilling, pit wall gradient change, pit migration rates and sediment characteristics, they lack the "ground truthing" that coring provides. For example, O'Connor (2017) used ^{7}Be penetration depths to estimate 12 – 34 cm of sediment deposition at Sandy Point over a period of ~ 100 days, which amounts to 0.44 – 1.24 m yr^{-1}. The lower estimate of this

infill rate agrees well with Obelcz et al. (2018), however, this illustrates the variability of sedimentation within BAs not captured by certain methodologies. Our study estimates volumetric infill for both Caminada and Sandy Point BA, which serves as a comparison to both numerical modeling and bathymetric data from the studies described above. Additionally, mass accumulation rates are also presented, which has not yet been attempted in these two study areas.

Upon excavation of sand at BA sites, sediment infills due to increased flow depth, which decreases flow velocity and allows sediment to settle from suspension (Nairn et al., 2005). Within the dredged area, areas that are deeper in comparison to the ambient pit depth (referred to as dredge scours) preferentially accumulate sediment more rapidly than the surrounding pit. These dredge scours have been described as uneven bathymetry within BAs left behind by dredging in both muddy and sandy seafloor settings (Liu et al., 2019; Robichaux et al., 2020). Once deeper areas have infilled, sediment typically begins to uniformly accumulate throughout the entire BA. For BAs with more constant sediment sources, deeper areas are quickly filled in (Obelcz et al., 2018; Robichaux et al., 2020). However, in sandy settings, dredge scours can persist for longer periods of time, most likely due to the lack of a constant source of sediment to infill them. At Caminada BA, for example, bathymetric surveys and coring have shown that fluvial sediment is preferentially accumulating within bathymetric low areas (Liu et al., 2019; Xue et al., *in review*; this study).

To estimate the total time to infill bathymetric lows within Caminada BA, ^{7}Be-derived sedimentation rates were seasonally averaged for coring work completed in September 2017 and May 2018 by Xue et al. (*in review*) as well as September 2018 in this study. A total of 8 bathymetric lows (shown in Fig 1) were mapped using bathymetric surveys taken for Caminada BA in August 2018 by Liu et al. (2019). The total area (m^2) of each bathymetric low was

calculated using ESRI ArcGIS's field calculator tool, which was then multiplied by the infill rate (m yr^{-1}) to obtain a volumetric infill rate. The results of this analysis are shown in Table 5. The volumetric infill rate for bathymetric lows within Caminada BA yielded a total time to infill between ~ 2 – 5 years. Volumetrically, bathymetric low areas are infilling ~ 78,000 m^3 yr^{-1}, significantly higher than the 27,500 m^3 yr^{-1} reported by Liu et al. (2019). As argued previously, low infill rates at Caminada is caused by the distance from fluvial-sediment sources. The sediment that does reach the BA is preferentially depositing within bathymetric lows, which explains why certain areas of Caminada contained no ^{7}Be-laden sediment. However, we found, ~ 2 cm of ^{7}Be-laden sediment was present at core Site 5 in September 2018 (Fig. 2), indicating this location has begun accumulating fluvially-derived sediment. Thus, it is possible that bathymetric lows in the eastern area of the pit (BL2, 3 and 4) have completely infilled, allowing sediment to uniformly blanket in the area surrounding Site 5 of the pit. At Sandy Point BA, topographic lows were not seen in bathymetric data from 2015 (via Obelcz et al., 2018), indicating that that the pit was a relatively uniform depth within ~ 3 years post-dredging. Thus, sedimentation rates were seasonally averaged for each coring site for July 2015 (O'Connor, 2017), May 2019 and September 2019 and subsequently extrapolated over the entire pit area (m^2) to obtain a volumetric infill rate (m^3 yr^{-1}). This analysis yielded an averaged volumetric infill rate of 235,000 m^3 yr^{-1} for Sandy Point BA, with a time to total infill of approximately 16 years. These results were in close agreement to the results presented above from Obelcz et al. (2018).

In addition to calculation of volumetric infill rates for Caminada and Sandy Point BAs, mass accumulation rates were also calculated. Mass accumulation rates were calculated by multiplying the averaged dry bulk density (kg m^{-3}) of multicores by the seasonally averaged infill

rates (m yr^{-1}). At Caminada, mass accumulation rate within the BA ranged from ~ 110 – 130 kg m^{-2} yr^{-1}. At Sandy Point, the mass accumulation rate within the pit ranged from ~ 280 – 430 kg m^{-2} yr^{-1}. Outside of each pit, no significant accumulations of recently deposited (< 6 months), fluvial-sediment were present in any coring survey (i.e., cores were ^{7}Be-dead). This data supports the notion that these BAs are sufficiently trapping fluvial-sediment that would otherwise be deposited elsewhere on the continental shelf, which has been discussed in detail in several studies (e.g., O'Connor, 2017; Obelcz et al., 2018; Robichaux et al., 2020).

Table 5. Calculated volume (m^3), infill rate (m^3 yr^{-1}), mass accumulation rate (kg m^{-2} yr^{-1}) and time to total infill (years) for bathymetric lows (BL) within Caminada BA using seasonally averaged infill rates.

BL	BL Area (m^2)	BL Volume (m^3)	BL Depth (m)	Nearest Core Site	Infill Rate (m^3 yr^{-1})	Mass Acc. Rate (kg m^{-2} yr^{-1})	Time to Total Infill (years)
1	144,000	115,000	0.8	CA2	30,000	111	3.8
2	52,000	21,000	0.4	CA4	11,000	126	1.9
3	74,000	30,000	0.4	CA4	16,000	126	1.9
4	11,000	4,600	0.4	CA4	2,400	126	1.9
5	21,000	21,000	1	CA3	4,500	130	4.8
6	38,000	38,000	1	CA3	8,000	130	4.8
7	11,000	11,000	1	CA3	2,300	130	4.8
8	19,000	15,000	0.8	CA3	4,000	111	3.8

BL depth estimated by taking the difference in depth between bathymetric lows and ambient pit depth (~ 12.5 m, Liu et al., 2019). Infill rate in kg m^{-2} $year^{-1}$ estimated using average dry bulk density (kg/m^3) of sediment cores collected from Caminada in September 2018 (See Fig. 1 for BL and coring locations).

Table 6. Calculated volume (m^3), infill rate (m^3 yr^{-1}), mass accumulation rate (kg m^{-2} yr^{-1}) and time to total infill (years) for the total pit area of Sandy Point BA using seasonally averaged infill rates.

Sandy Point BA	Core Site	Infill Rate (m yr^{-1})	Infill Rate (m^3 $year^{-1}$)	Mass Acc. Rate (kg m^{-2} yr^{-1})	Time to Total Infill (years)
Total Pit Volume (m^3)	SP1	0.96	386,000	431	10
3.7×10^6	SP2	0.39	158,000	182	24
	SP3	0.37	148,000	156	25
	SP5	0.62	248,000	277	15
Averaged for all Sites		0.58	235,000	261	16
Obelcz et al. (2018)			200,000		15

Infill rate in kg m^{-2} $year^{-1}$ estimated using average dry bulk density (kg/m^3) of sediment cores collected from Sandy Point in May 2019 (See Fig. 1 for coring locations).

Results from our study at Caminada and Sandy Point BA reveal that sediment infill is accumulating at rates differing from numerical modeling proposed by Nairn et al. (2005). For

instance, modeling of sandy pit evolution in a setting similar to Caminada BA revealed total infill of material transported via bedload within 5 years, however, our study concludes that even the small bathymetric lows (40 – 100 cm deeper compared to ambient pit depth) will not be entirely filled until ~ 5 years post-dredging. Furthermore, our results show the material at Caminada consists almost entirely of far-field, fluvial sediment (i.e., Type 1 and 3) during summer months and resuspended sediment flushed from the continental shelf and bays following winter storms (i.e., Type 2 sediment; Table 4). Due to this, a new conceptual model for the evolution of sandy borrow areas based on observations from previous studies (Liu et al., 2019; Xue et al., *in review*) and this study is presented here, as shown in Figure 12. Within our model, pit evolution is separated into 3 main phases. Stage 1 occurs in the days to months immediately following excavation in 2017. During this phase, we assume that pit walls rapidly equilibrated to sub-annual scale forcings such as tidal fluctuations and storms. This phase was also proposed for Sandy Point BA by Obelcz et al. (2018), however, the resultant infill from pit wall equilibration was higher (~ 10% total pit infill) than what is seen at Caminada BA (< 3 percent; Liu et al., 2019 and ~ 7% for Site 4; this study). Stage 2 occurs ~ 1 – 5 years post-dredging and consists of total infill of bathymetric lows until sediment begins blanketing across the entire pit. During stage 2, pit infill is dominated by fluvial and shelf resuspension-derived sediments, as pit walls are less failure prone once they have equilibrated to sub-annual forcings (Obelcz et al., 2018). Further, stage 2 evolution at Caminada BA differs from Sandy Point, as topographic lows are more persistent. Stage 3 represents the time to completely infill the pit after bathymetric lows have completely infilled. This time to infill was calculated by using high and low sedimentation rate averaged from multiple studies (e.g., Liu et al., 2019; Xue et al., in review; this study) extrapolated over the area of the pit, which yielded a volumetric infill rate of ~ 110,000 $m^3\ yr^{-1}$,

significantly greater than the 27,380 m^3 yr^{-1} calculated by Liu et al. (2019). Dividing the remaining pit volume of Caminada BA after topographic lows have been filled yielded a time to infill of approximately 60 years, assuming constant sedimentation. For comparison, the infill rate from Liu et al. (2019) yielded a much longer time to infill of approximately 230 years. However, it is likely that the time to total infill in sandy settings will be lessened by the passage of tropical storm and hurricane systems, which are assumed to cause rapid infill in BAs located in muddy hydrodynamic settings (e.g., Robichaux et al., 2020; this study).

For Sandy Point BA, numerical modeling completed by Nairn et al. (2005) concluded that the pit would infill within 10 years post-dredging, sourced mainly from suspended sediment exiting the Mississippi River delta and local seabed resuspension. Results from our study agree with the two main sources of sediment, however, we observed strong seasonal variation in infilling rate not predicted by the Nairn model. This seasonal variation not accounted for in the model leads to an underestimation of the time to infill the entire pit, as shown in Figure 13 below. Based on ^{7}Be-dervied infill rates, we conclude that infilling is much more varied in settings where a proximal seasonal sediment source exists (i.e., discharge dependent). Based on our updated sedimentation rates, we predict that Sandy Point BA will take ~ 15 – 20 years to infill completely (Table 6; Fig 13). In order to improve upon modeling of BAs in muddy seafloor settings, future efforts could focus on adding an additional component to account for seasonal variation in sediment discharge.

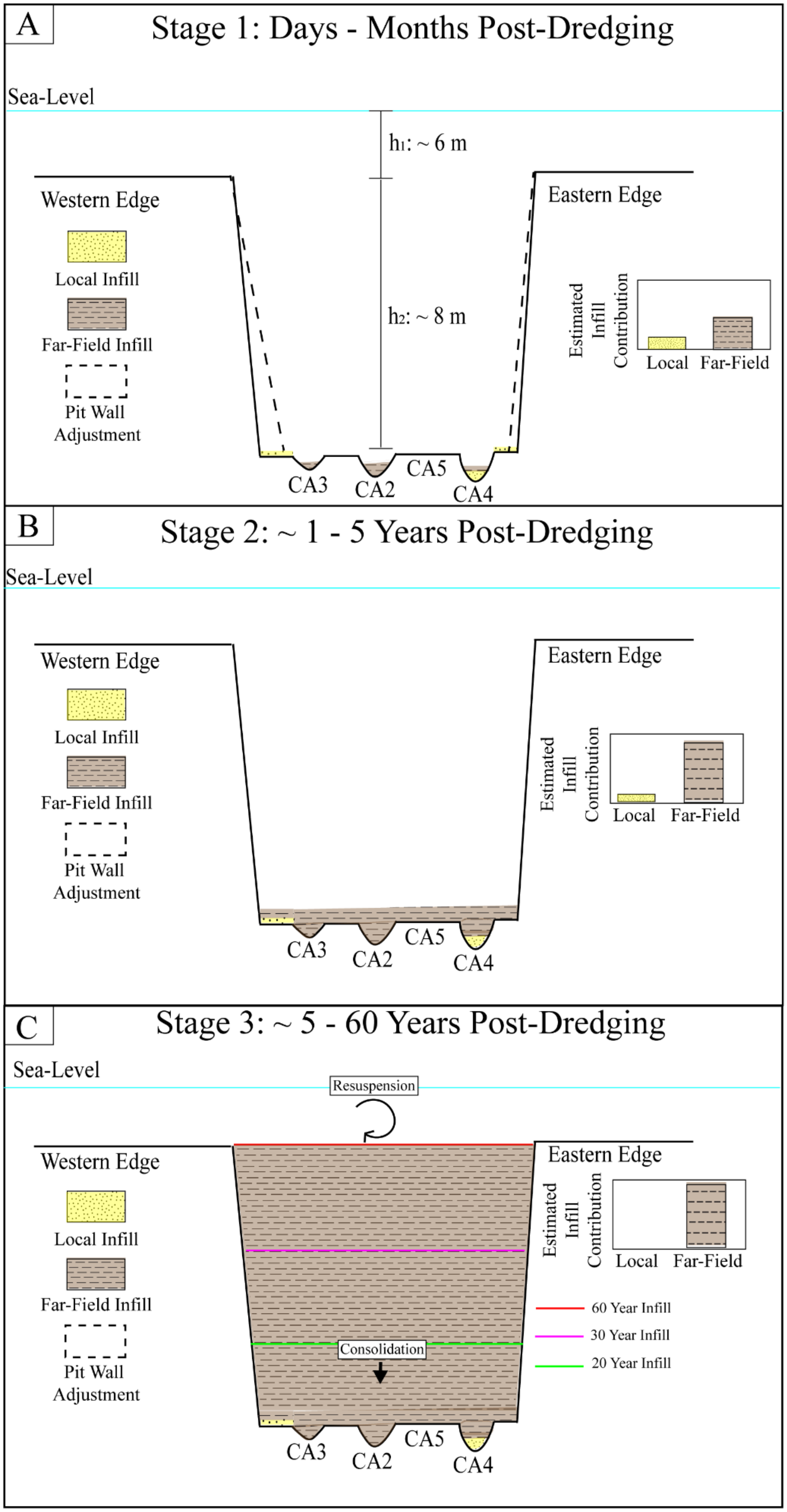
A
Stage 1: Days - Months Post-Dredging
Sea-Level
h1: ~ 6 m
h2: ~ 8 m
Western Edge
Eastern Edge
Local Infill
Far-Field Infill
Pit Wall
Adjustment
Estimated
Infill
Contribution
Local
Far-Field
CA3
CA2
CA5
CA4
B
Stage 2: ~ 1 - 5 Years Post-Dredging
Sea-Level
Western Edge
Eastern Edge
Local Infill
Far-Field Infill
Pit Wall
Adjustment
Estimated
Infill
Contribution
Local
Far-Field
CA3
CA2
CA5
CA4
C
Stage 3: ~ 5 - 60 Years Post-Dredging
Sea-Level
Resuspension
Western Edge
Eastern Edge
Local Infill
Far-Field Infill
Pit Wall
Adjustment
Estimated
Infill
Contribution
Local
Far-Field
60 Year Infill
30 Year Infill
20 Year Infill
Consolidation
CA3
CA2
CA5
CA4

Figure 12 (Previous Page). Conceptual model for infilling at Caminada BA separated into 3 phases (modified from Obelcz et al., 2018, Model not to scale). (A): Phase 1 of evolution, hypothesized to take place days to ~ 1-year post dredging. In this phase, pit walls adjust, depositing minor amounts of local sediment within the BA. Sediment also begins accumulating within bathymetric lows. (B): Phase 2, hypothesized to take place ~ 1 – 5 years post-dredging. During this phase, topographic lows are filled by far-field and winter-storm (Type 1,2, 3) sediments, with minimal local infill (Type 4) contribution, allowing sediment to accumulate uniformly across the entire pit. (C): Phase 3, hypothesized to take place ~ 5 – 50 years post-dredging. Sediment accumulates and begins consolidating under its own weight. It is likely that storm induced transport could accelerate the infill during this stage.

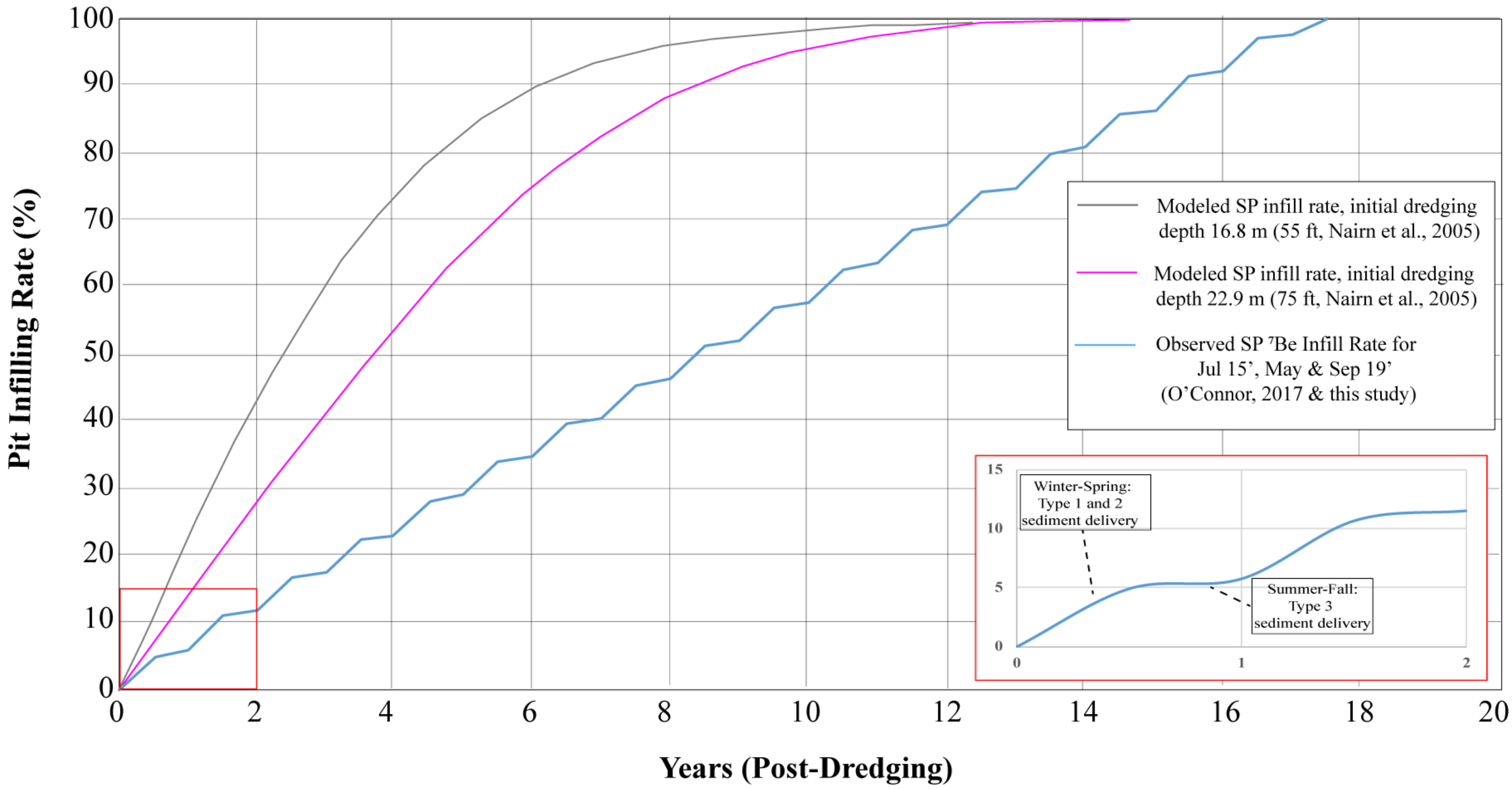

Figure 13. Modeled infill rates from Nairn et al.(2005) for Sandy Point Infill, assuming different initial dredging depths, shown in pink and gray, versus observed infill rate derived from ^{7}Be in this study (blue). The area boxed in red is enlarged in the bottom-right to show the strong seasonal variation in infill rate and observed sediment types from repeat coring surveys.

5.4. Implications to Coastal Restoration and Future Work

Repeat coring and bathymetric surveys at both Caminada and Sandy Point BA suggest that sediment infill is characteristically different from the material dredged from these locations. Specifically, grain size and radiochemical analysis from this study support findings from Xue et

al. (*in review*) that there is an evident lack of ambient Ship Shoal sand within the infilled material inside the borrow area, which is contrary to proposed models from Nairn et al. (2005). Further, Caminada BA is infilling much more slowly (~ 10 times) than predicted by numerical modeling from (Nairn et al., 2005) and ~ 4 times quicker than volumetric infill rates from Liu et al. (2019). Caminada BA sedimentation rates display seasonality, although to a lesser extent than Sandy Point (0.02 – 0.2 cm day^{-1} at Sandy Point versus 0.3 – 0.10 cm day^{-1} at Caminada from fall to spring, respectively). Further, analysis of Sandy Point BA cores recovered in September 2019 reveals rapid infill of ~ 0.3 – 0.5 meters of sediment derived from resuspended material from the ambient seafloor surrounding the pit following the passage of Hurricane Barry (i.e., Type 5 sediment). Based on core analysis of sediments containing ^{7}Be and grain size presented in this study, our results support findings from previous work at both Caminada (Liu et al., 2019; Xue et al., in review) and Sandy Point (O'Connor 2017; Obelcz et al., 2018) that the majority of sediment infill is fluvial-derived (Type 1 and 3) from the Mississippi and Atchafalaya Rivers (~ 30 % at Caminada, ~ 80% at Sandy Point). Additionally, we conclude that winter storms contribute more to annual infill at Caminada (~ 66 – 73 %) compared to Sandy Point (~ 12 – 20 %) due to the greater distance from a fluvial-sediment source (Table 4).

The data presented here suggests that repeat surveys are needed at Caminada to understand how a persistent bathymetric depression within Ship Shoal will impact water quality, biogeochemistry and benthic communities within this area. Additionally, future coring at Caminada BA could be completed following the passage of hurricanes, in order to understand if ambient Ship Shoal sediment is infilling following extreme weather, similar to what was observed at Sandy Point in this study. Our data also provide evidence that numerical modeling in both sandy and muddy settings needs to be updated to include the influence of seasonal

discharge variations of the Mississippi and Atchafalaya Rivers, as well as rapid infill events caused by low frequency, high magnitude events such as hurricanes. Furthermore, due to both BAs infilling with finer-grained sediments, sandy shoal and buried paleochannel restoration-quality sand resources are not renewable in these locations.

Conclusion

1) In fall 2018, 2 – 6 cm of ^{7}Be-laden sediments were deposited Caminada BA. Sedimentation rates were calculated to be 0.02 – 0.04 cm day^{-1}. On average, the sediment infill has a median grain size around fine- to coarse-silt, ranging from 12 - 45 μm (4.5 – 6.5 Φ). In May 2019, approximately 14 – 34 cm of ^{7}Be-laden sediments were deposited within ~ 6 months at Sandy Point BA. Sedimentation rates were calculated to be 0.1 – 0.5 cm day^{-1}. During repeat coring in September 2019, only 2 – 6 cm of ^{7}Be-laden sediment were deposited, and sedimentation rates were 0.02 – 0.03 cm day^{-1}. There is little difference between median grain size of 6.0 – 8.5 μm (~ 7 Φ) between the two coring surveys.
2) For Sandy Point BA cores, we identified Type 1, 2 and 3 sediment packages as described by O'Connor (2017), as well as a new (Type 5) sediment not previously seen within the BA, inferred to represent rapid deposition following Hurricane Barry. Type 3 sediment identified here had higher ^{7}Be activity (~ 2 – 6 dpm g^{-1}) compared to O'Connor (2017; ~ 1.5 dpm g^{-1}). At Caminada BA, we also observe Type 2 and 3 units in the dredge pit infill, along with a new sedimentary package that we describe as Type 4. Type 2 sediment packages were on average thicker than those identified at Sandy Point BA (~ 8 cm versus ~ 4 cm on average). Type 3 sediment identified here had higher ^{7}Be activity (~ 4 – 13 dpm g^{-1}) than those identified at Sandy Point BA due to timing of the coring relative to high discharge from the rivers. Finally, the newly defined Type 4 sediment consisted of thin (1 - 2 cm) fine sand layers with no ^{7}Be activity (exemplified in CA4 for September 2018 in Fig 6), inferred to represent local infill from pit wall failure/readjustment.

3) Our results indicate that winter storms deposited ~ 12 – 20% of the annual infill seen within Sandy Point cores collected in May 2019. In comparison, we estimate that ~ 66 – 73% of annual infill within Caminada BA cores collected in May 2018 was from winter storms. We attribute the greater portion of Type 2 sediment relative to annual infill at Caminada to the lack of proximal fluvial-sediment source at this BA. Analysis of cores recovered at Sandy Point BA in September 2019 revealed 0.3 – 0.5 m of ^{7}Be-dead sediment with a distinct bimodal distribution seen in grain size that fines upward and appears as low density, massive beds of sediment with brighter basal layers in x-radiographs, which we interpret to be deposited following Hurricane Barry.
4) Volumetric analysis of infill at Caminada and Sandy Point yielded significantly different times to total infill from those predicted by Nairn et al. (2005). For Caminada, we predict the pit will infill within ~60 years, slower than the 5 years predicted by Nairn's model for sandy dredge pits and more quickly than volumetric analysis from Liu et al. (2019) suggests. Our results indicate Sandy Point is infilling ~ 235,000 m^3 yr^{-1}, with a time to total infill of ~ 15 – 20 years. Further research is needed to better understand how hurricanes affect BA sedimentation in sandy settings along the Louisiana Coast, and how a persistent bathymetric depression will impact the Ship Shoal area.

Appendix A. Individual ^{7}Be Activity (dpm g^{-1}) versus depth (cm) Plots

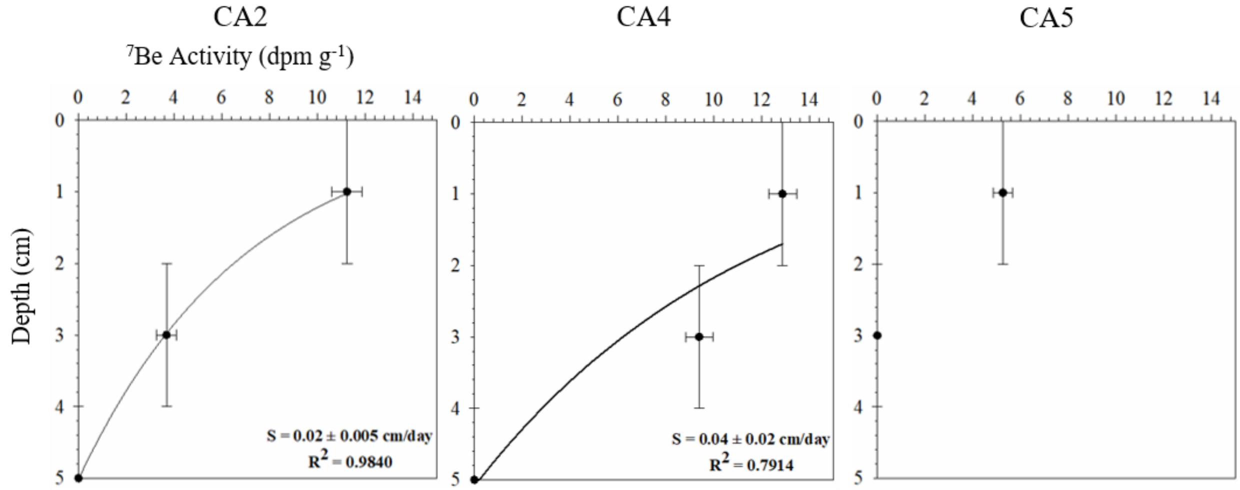

A.1. ^{7}Be Activity (dpm g^{-1}) versus depth (cm) for Caminada multicores recovered in September 2018. No ^{7}Be activity was found at depth in cores X-Y.

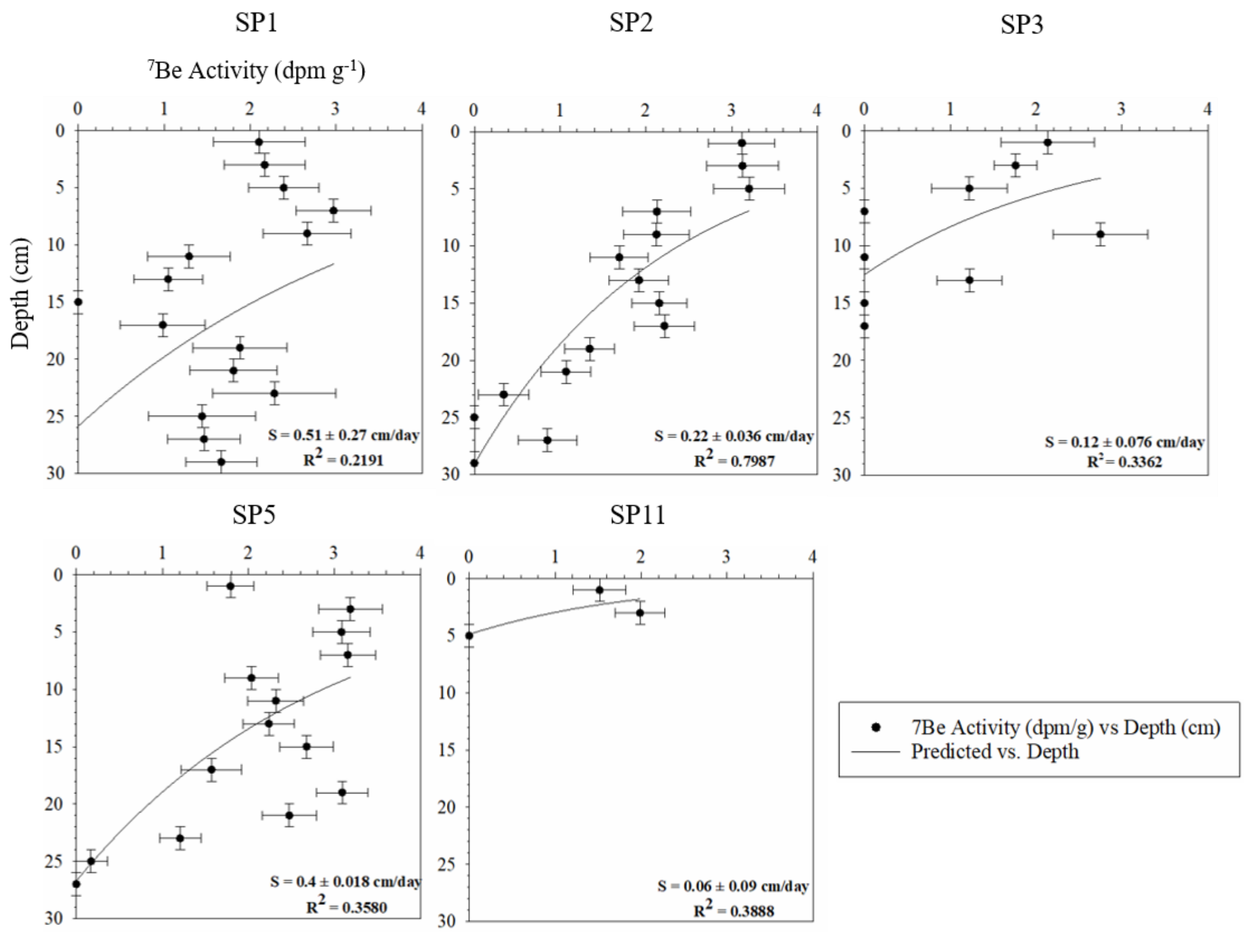

A.2. ^{7}Be Activity (dpm g^{-1}) versus depth (cm) for Sandy Point multicores recovered in May 2019

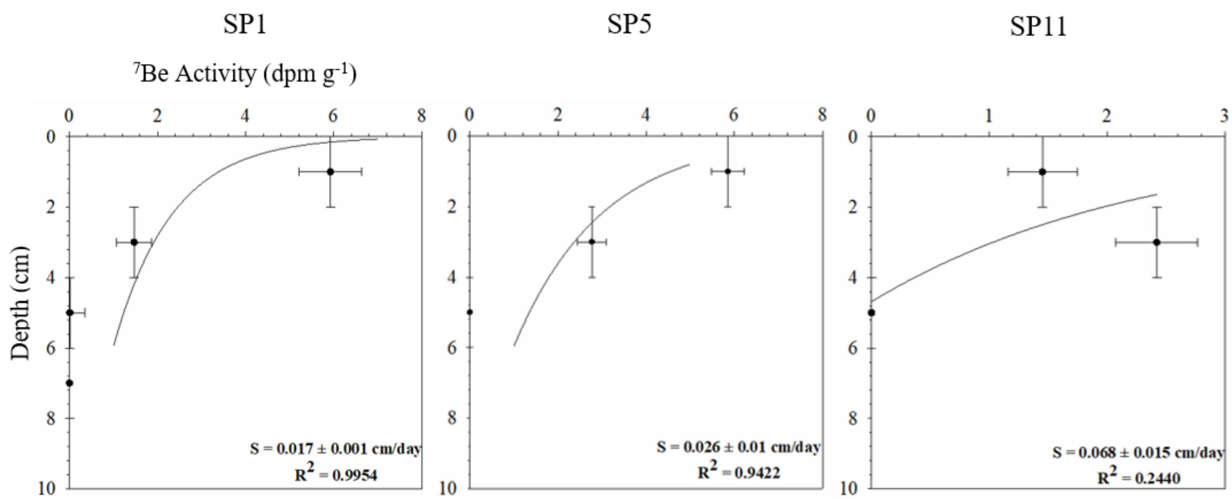

A.3. ^{7}Be Activity (dpm g^{-1}) versus depth (cm) for Sandy Point multicores recovered in September 2019. No ^{7}Be activity was found at depth in cores X-Y.

Appendix B. Individual Grain Size Frequency Contour Plots

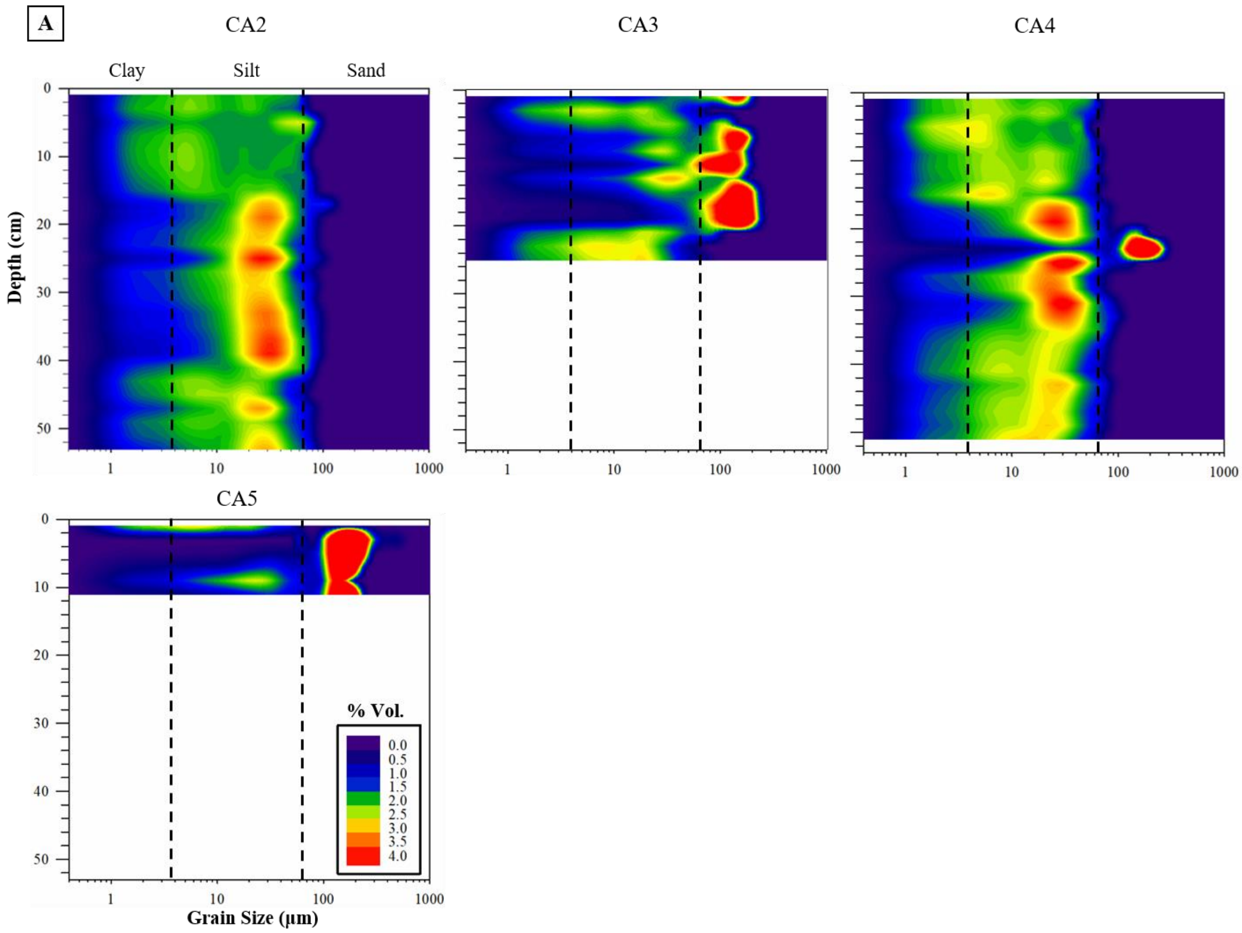

B.1. Grain Size frequency contour plots for Caminada cores collected September 2018

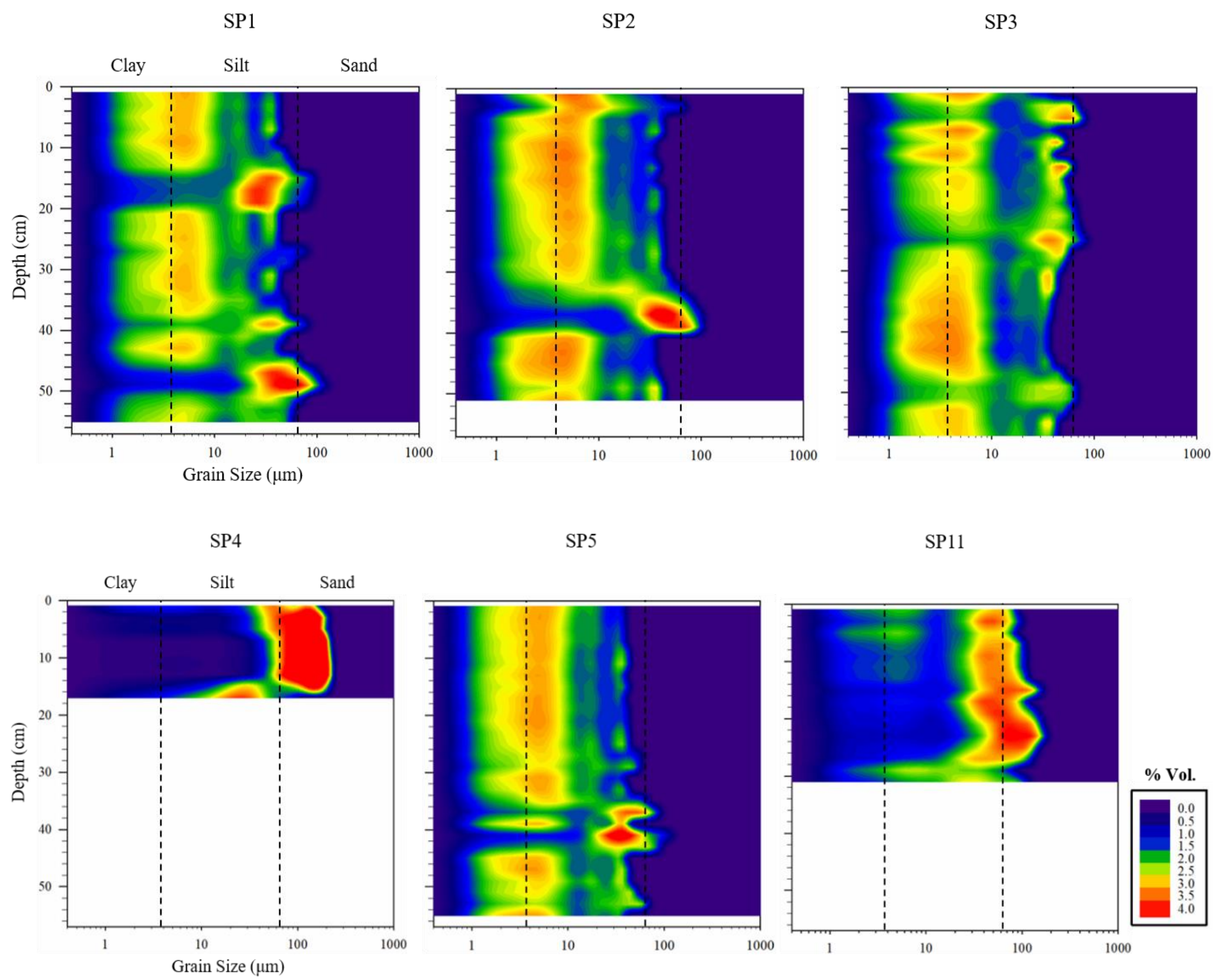

B.2. Grain Size frequency contour plots for Sandy Point cores collected May 2019

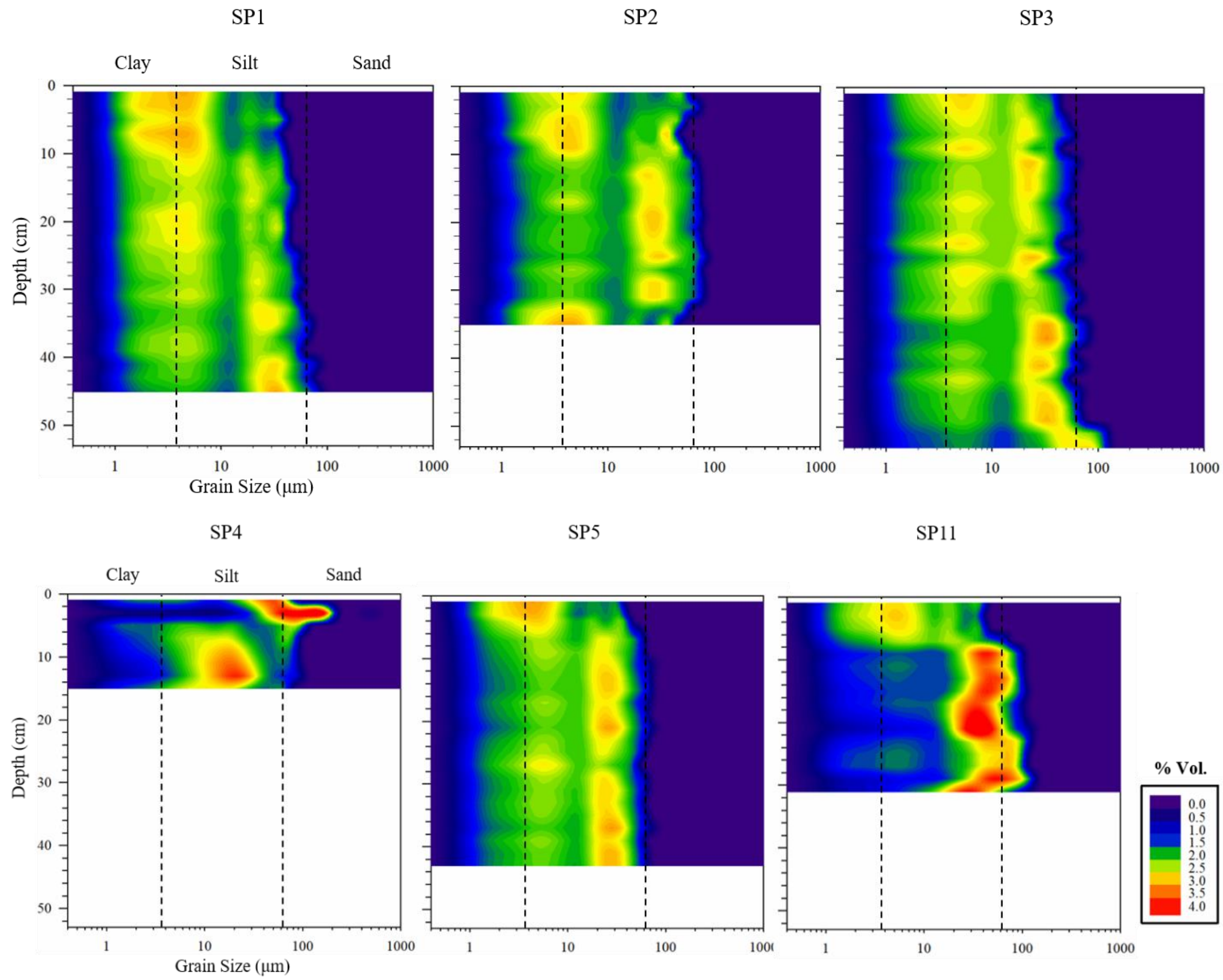

B.3. Grain Size frequency contour plots for Sandy Point cores collected September 2019

Appendix C. Unannotated X-radiographs

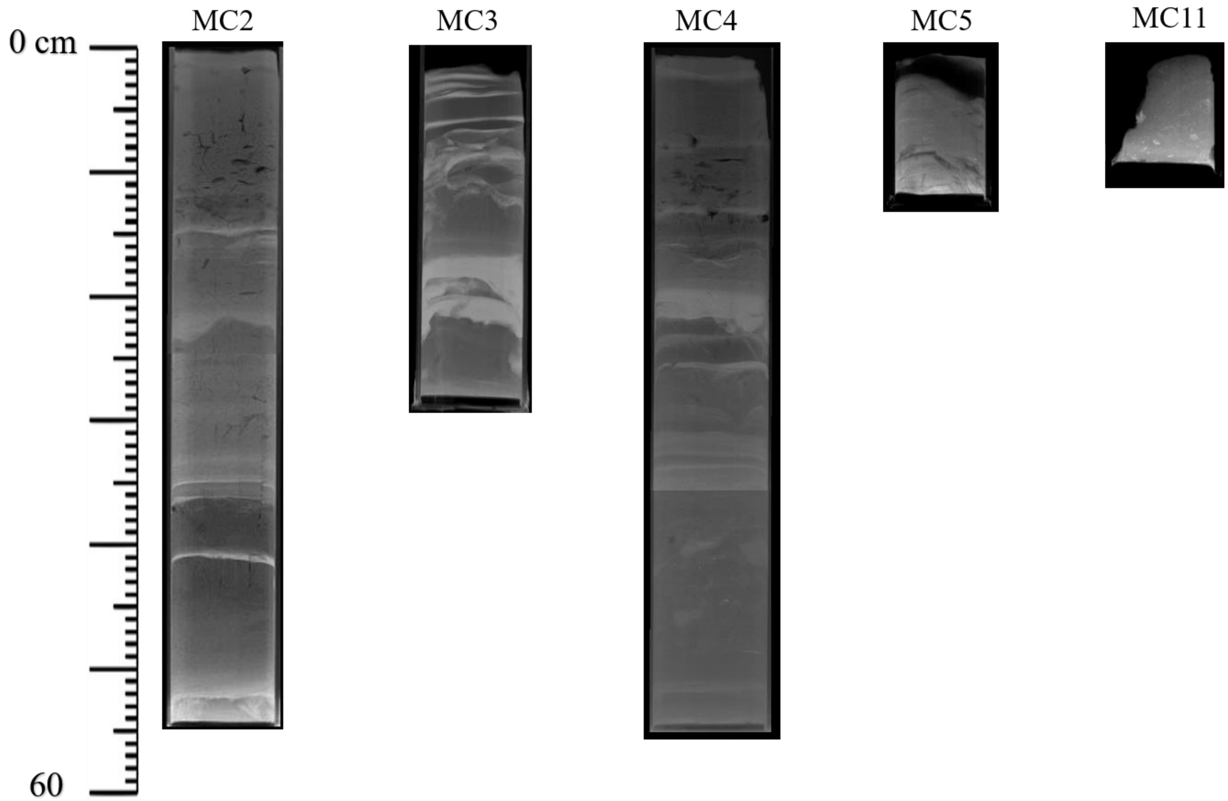

C.1. X-radiographs for Caminada September 2018

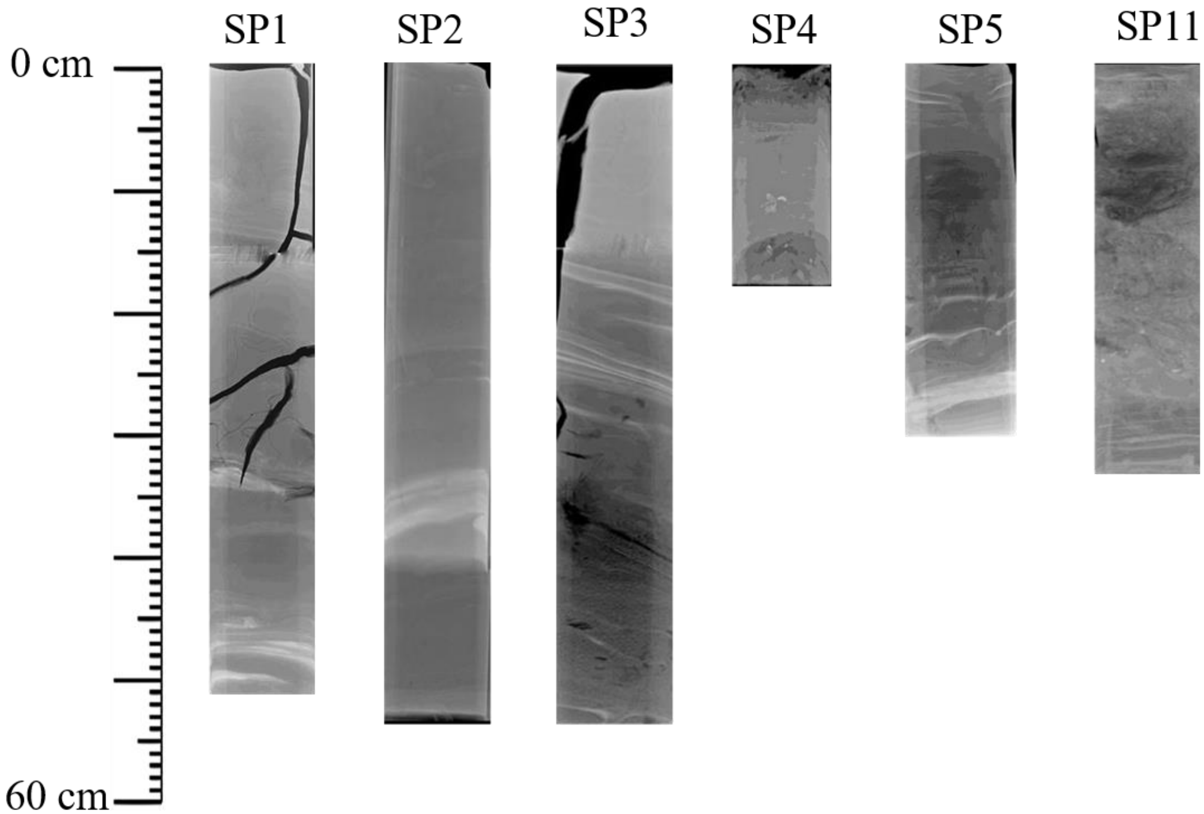

C.2. X-radiographs for Sandy Point May 2019

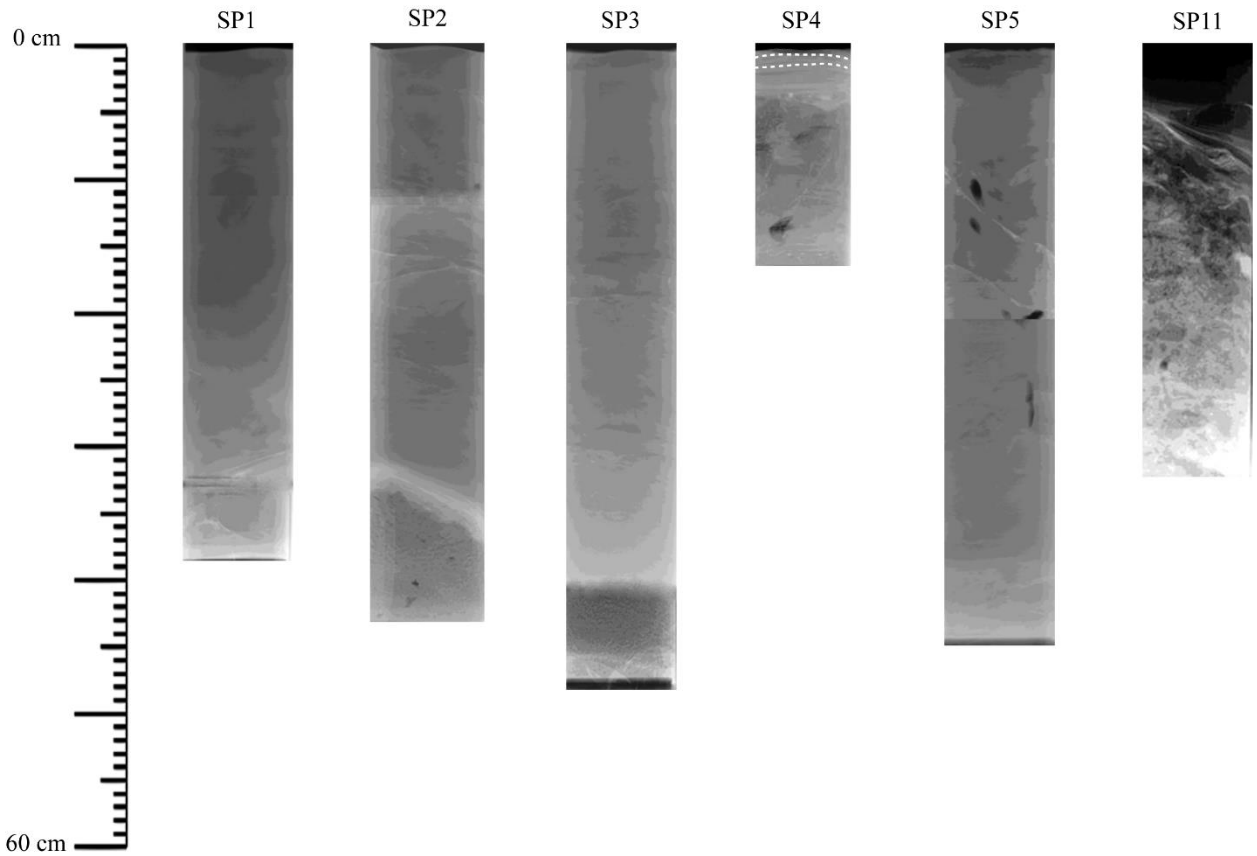

C.3. X-radiographs for Sandy Point September 2019

Appendix D. Meteorological Data for coastal Buoy CSI-06 (A, B, and C) and BURL-1 (D)

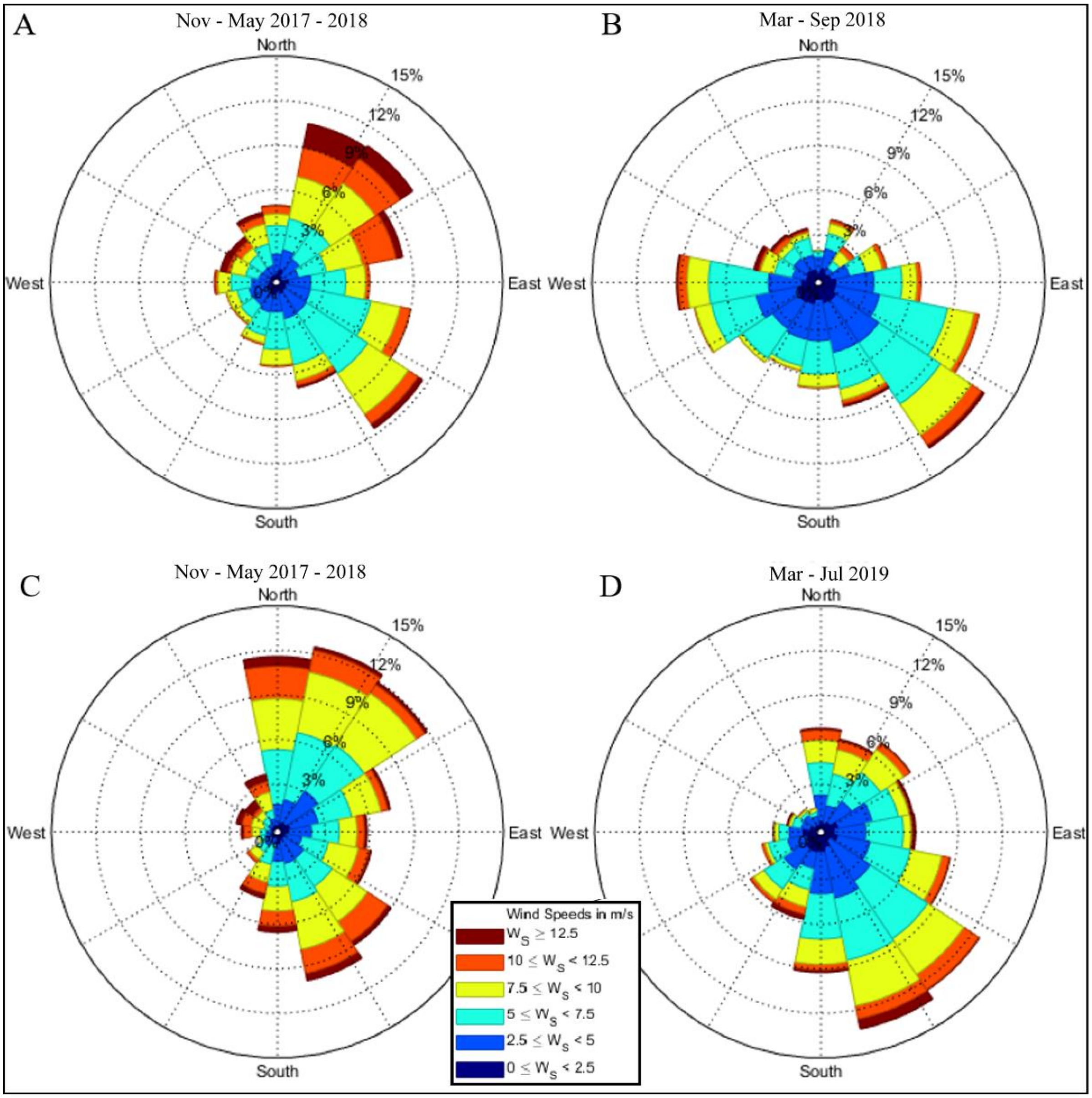

D.1. Wind rose diagrams for ~ 6 months prior to field sampling dates.

Appendix E. Reclassified MODIS Imagery. Imagery downloaded from LSU's Earth Scan Laboratory

E.1. January 5th, 2019

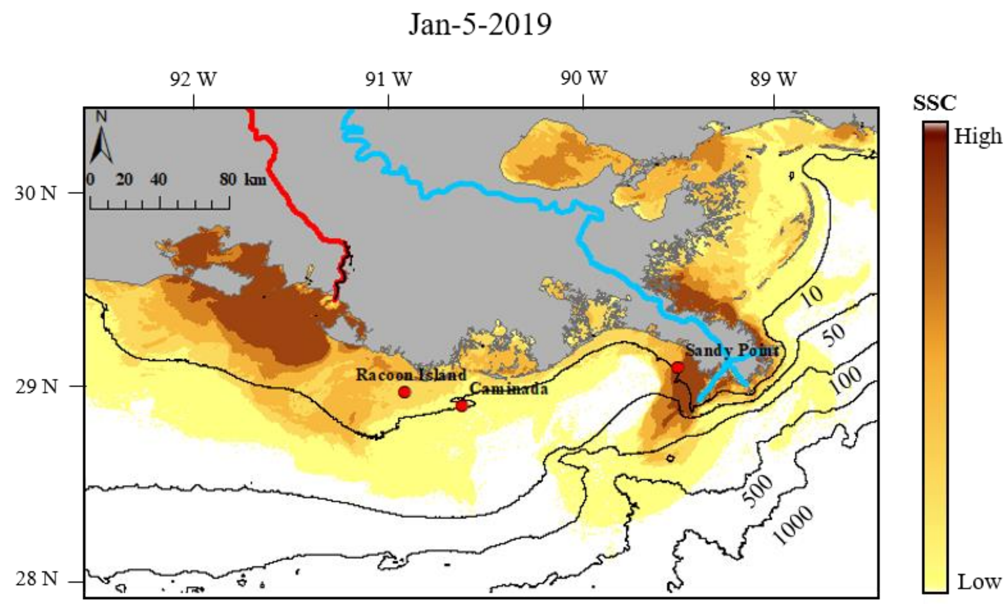

E.2. January 6th, 2019

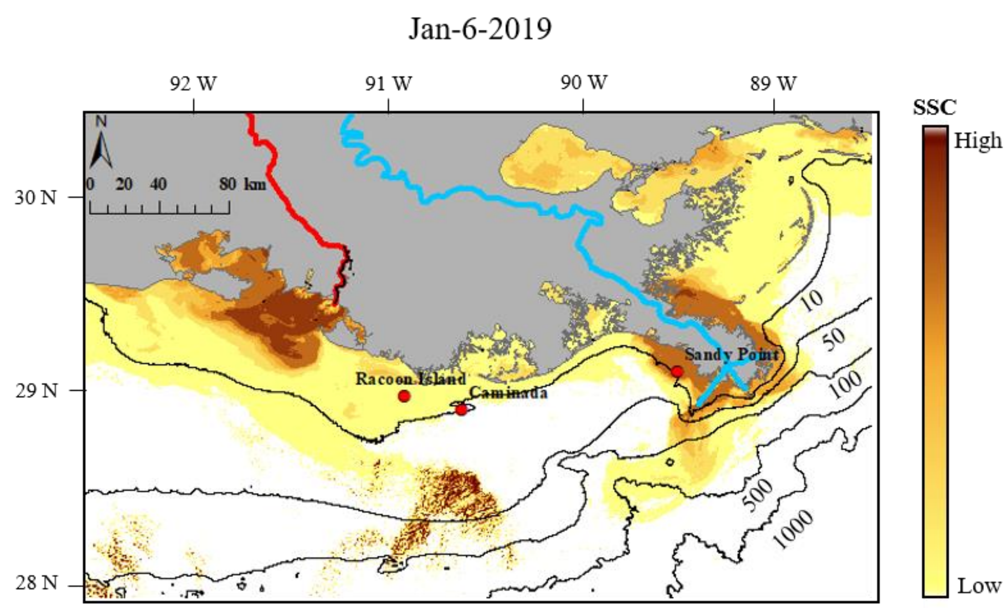

E.3. January 10th, 2019

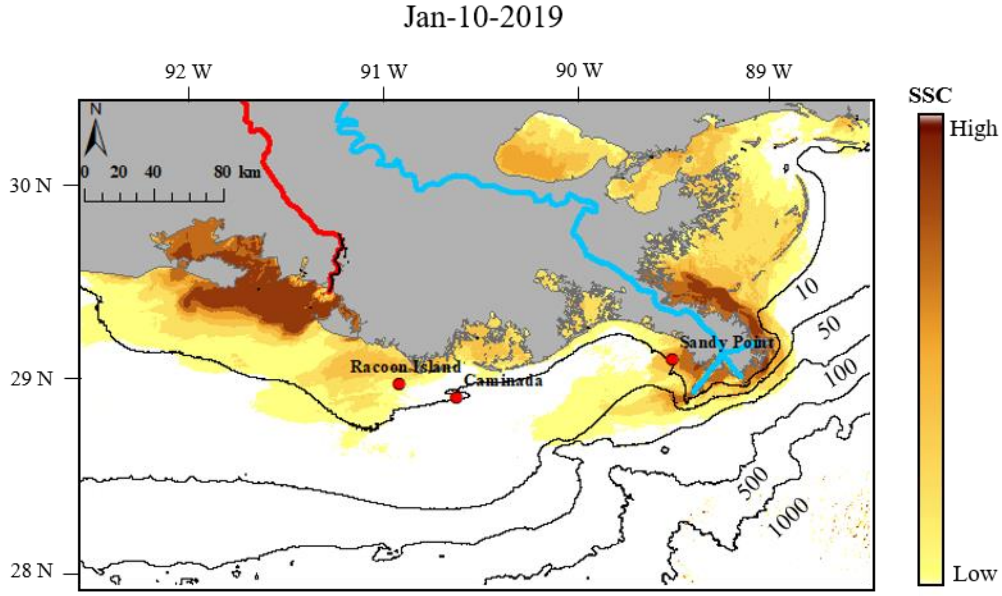

E.4. April 10th, 2019

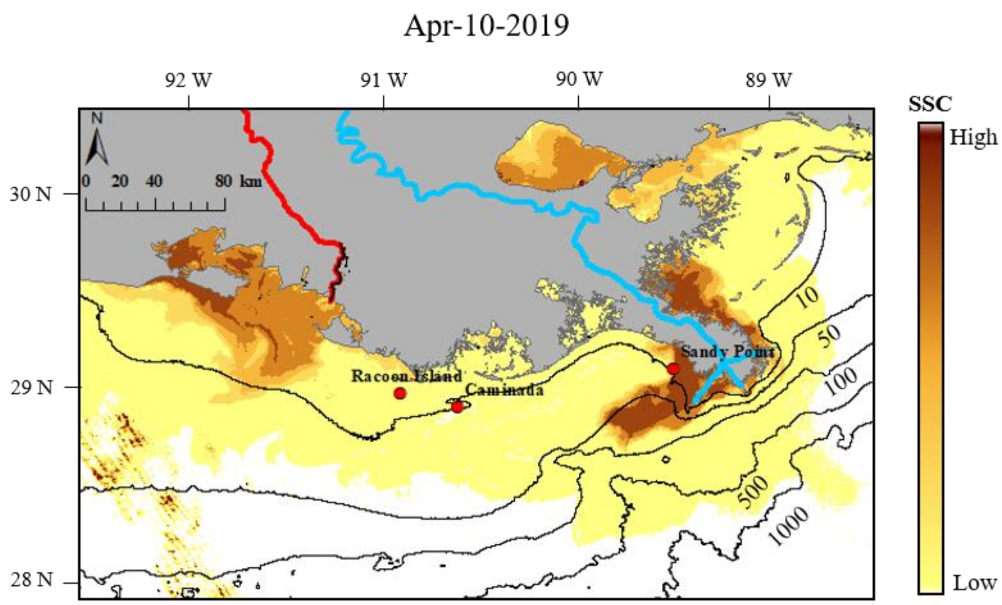

E.5. April 20th, 2019

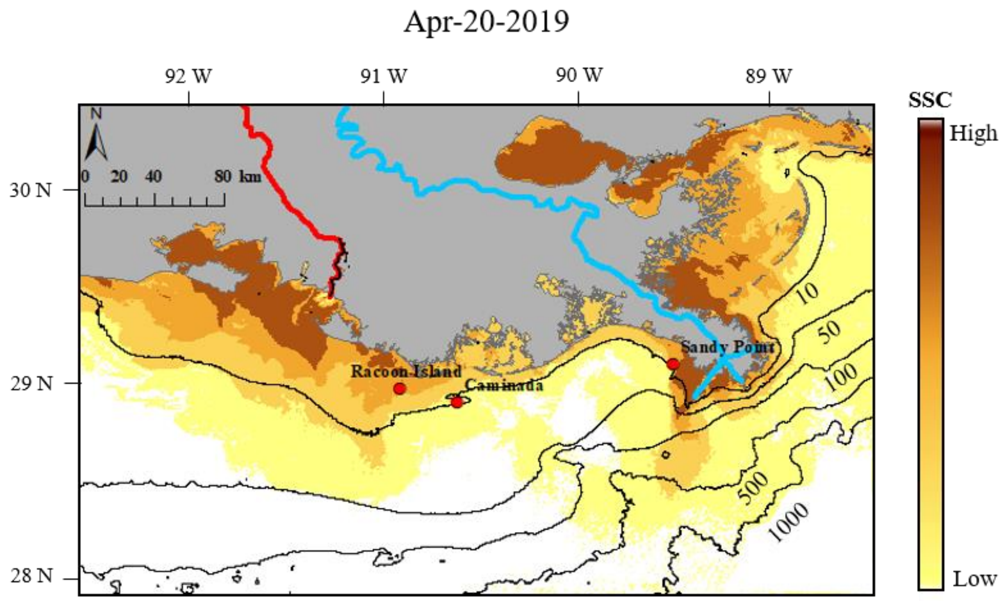

E.6. April 25th, 2019

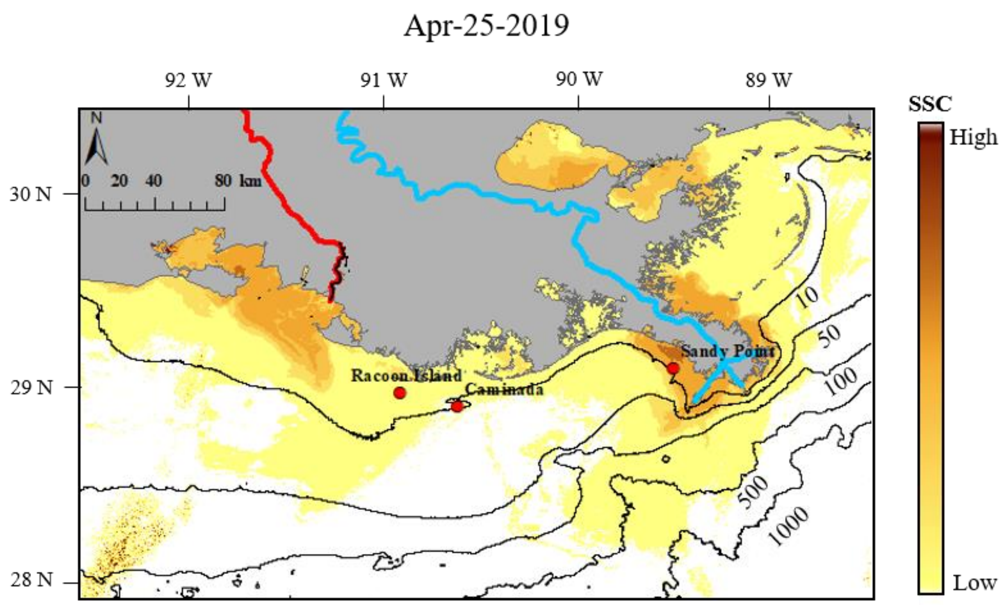

E.7. April 26th, 2019

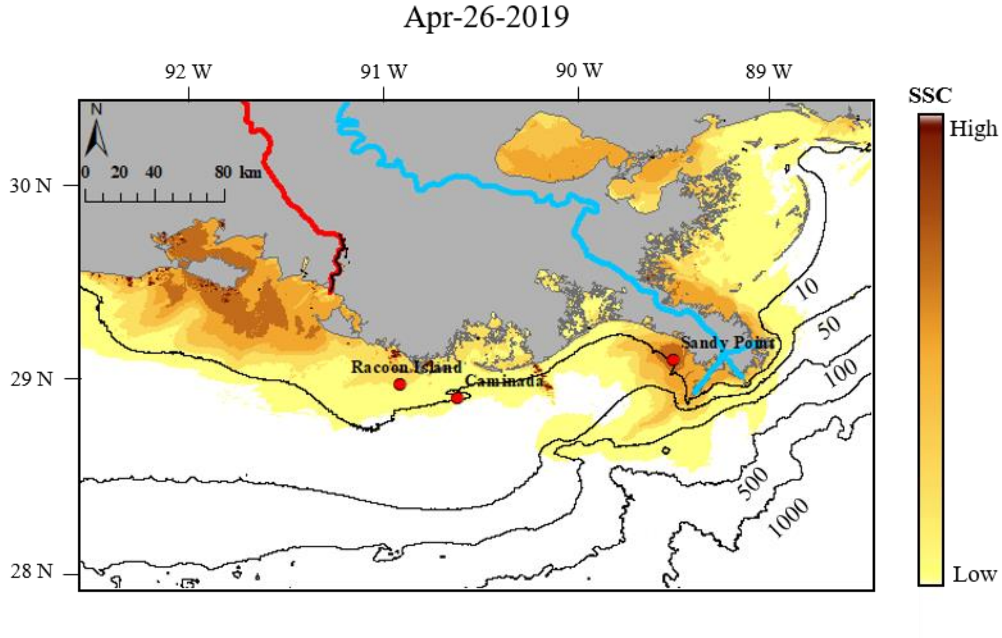

Appendix F. USSEABED Interpolated Mud Fraction for the northern Gulf of Mexico

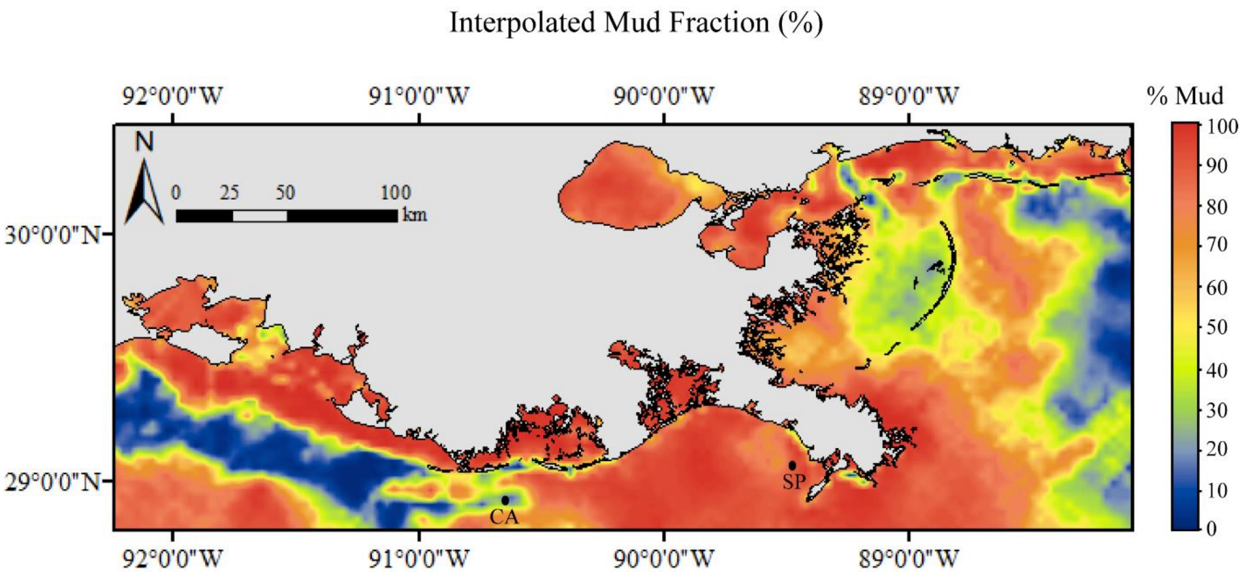

F.1. Interpolated Mud Fraction Map

Appendix G. Time to Infill Versus Volume Excavated for U.S. Borrow Areas.

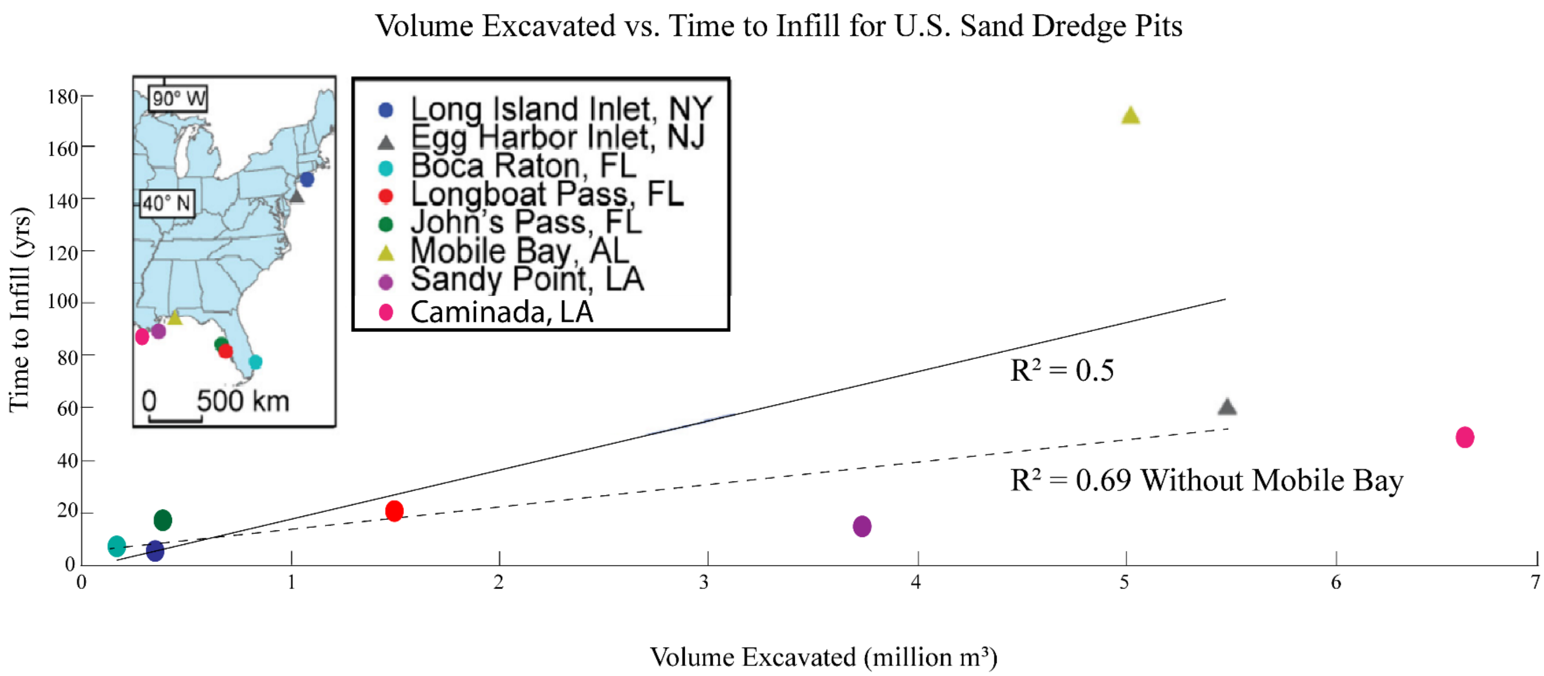

G.1. Time to Infill for US Borrow Areas (Modified from Obelcz et al., 2018)

References

Allison, M.A., Sheremet, A., Goni, M.A., Stone, G.W., 2005. Storm layer deposition on the Mississippi-Atchafalaya subaqueous delta generated by Hurricane Lili in 2002. Continental Shelf Research 25, 2213–2232.

Allison, M. A., C. R. Demas, B. A. Ebersole, B. A. Kleiss, C. D. Little, E. A. Meselhe, N. J. Powell, T. C. Pratt and B. M. Vosburg (2012). "A water and sediment budget for the lower Mississippi–Atchafalaya River in flood years 2008–2010: implications for sediment discharge to the oceans and coastal restoration in Louisiana." Journal of Hydrology 432: 84-97.

Bales et al. (*in prep)*, Hydrodynamics, Sediment Transport, and Water Quality of Two Contrasting Dredge Pits of Louisiana Shelf, LSU Thesis

Baskaran, M., Coleman, C.H. and Santschi, P.H., 1993. Atmospheric depositional fluxes of 7Be and 210Pb at Galveston and College Station, Texas. Journal of Geophysical Research: Atmospheres, 98(D11), pp.20555-20571.

Bender, M. A., T. R. Knutson, R. E. Tuleya, J. J. Sirutis, G. A. Vecchi, S. T. Garner, and I. M. Held (2010), Modeled impact of anthropogenic warming on the frequency of intense Atlantic hurricanes, Science, 327, 454–458, doi:10.1126/science.1180568

Bentley S.J., 2002, Dispersal of fine sediments from river to shelf: process and product.

Bentley, S.J., Keen, T.R., Blain, C.A. and Vaughan, W.C., 2002. The origin and preservation of a major hurricane event bed in the northern Gulf of Mexico: Hurricane Camille, 1969. Marine Geology, 186(3-4), pp.423-446.

Buczkowski, B.J., Reid, J.A., Jenkins, C.J., Reid, J.M., Williams, S.J., Flocks, J.G., 2006. usSEABED: Gulf of Mexico and Caribbean (Puerto Rico and U.S. Virgin Islands) offshore surficial sediment data release: U.S. Geological Survey Data Series 146, version 1.0. Available at: ⟨http://pubs.usgs.gov/ds/2006/146/⟩.

Chaichitehrani, Nazanin, et al. “A Numerical Study of Sediment Dynamics over Sandy Point Dredge Pit, West Flank of the Mississippi River, during a Cold Front Event.” *Continental Shelf Research*, vol. 183, 2019, pp. 38–50., doi:10.1016/j.csr.2019.06.009

Coleman JM, Prior DB, Garrison LE (1980) Subaqueous sediment instabilities in the offshore Mississippi River delta. Open File Report 80- 02. US Department of the Interior, Bureau of Land Management

Corbett, D., Mckee, B., & Duncan, D. (2004). An evaluation of mobile mud dynamics in the Mississippi River deltaic region. Marine Geology, 209(1-4), 91-112.

Costanza, R.; P´erez-Maqueo, O.; Martinez, M.L.; Sutton, P.; Anderson, S.J., and Mulder, K., 2008. The value of coastal wetlands for hurricane protection. Ambio, 37, 241–248.

Couvillion, B.R., Beck, H, Schoolmaster, D, and Foster, M, 2017. Land Area Change in Coastal Louisiana (1932 to 2016), US Department of the Interior, US Geological Survey.

CPRA (Coastal Protection and Restoration Authority), 2012. Louisiana's Comprehensive Master Plan for a Sustainable Coast. Baton Rouge, Louisiana: CPRA, 188p

Day, J.W., Jr, Boesch D.F., Clairain EJ, Kemp GP, Laska SB, Mitsch WJ, Orth K, Mashriqui H, Reed DR, Shabman L, Simenstad CA, Streever BJ, Twilley RR, Watson CC, Wells JT, Whigham DF (2007) Restoration of the Mississippi Delta: lessons From hurricanes Katrina and Rita. Science 315:1679–1684

Demas, C.R., Curwick, P.B., 1988. Suspended-sediment and associated chemical transport characteristics of the lower Mississippi River, Louisiana. Louisiana Dept. Transportation Develop. Water Resoures. Tech. Rep. 45 (44 pp).

Elgar, S., Raubenheimer, B., 2008. Wave dissipation by muddy seafloors. Geophys. Res. Lett. 35 (7).

Kaste, J. M., & Baskaran, M. (2011). Meteoric 7Be and 10Be as Process Tracers in the Environment. Handbook of Environmental Isotope Geochemistry, 61-85.

Feagin, R.A.; Mukherjee, N.; Shanker, K.; Baird, A.H.; Cinner, J.; Kerr, A.M.; Koedam, N.; Sridhar, A.; Arthur, R.; Jayatissa, L.P.; Lo Seen, D.; Menon, M.; Rodriguez, S.; Shamsuddoha, M., and Dahdouh-Guebas, F., 2010. Shelter from the storm? Use and misuse of coastal vegetation bioshields for managing natural disasters. Conservation Letters, 3, 1–11.

Fisk, H. N., Kolb, C. R., Mcfarlan, E., & Wilbert, L. J. (1954). Sedimentary framework of the modern Mississippi delta [Louisiana]. *Journal of Sedimentary Research*, *24*(2), 76–99. doi: 10.1306/d4269661-2b26-11d7-8648000102c1865d

Flocks, James, et al. "Evolution and Preservation Potential of Fluvial and Transgressive Deposits on the Louisiana Inner Shelf: Understanding Depositional Processes to Support Coastal Management." *Geo-Marine Letters*, vol. 29, no. 6, 2009, pp. 359–378., doi:10.1007/s00367-009-0164-4.

Gedan, K.B.; Kirwan, M.L.; Wolanski, E.; Barbier, E.B., and Silliaman, B.R., 2011. The present and future role of coastal wetland vegetation in protecting shorelines: answering recent challenges to the paradigm. Climatic Change, 106(1), 7–29.

Goni, M.A., Gordon, E.S., Monacci, N.M., Clinton, R., Gisewhite R., Allison, M.A., Kineke, G., 2006. The effect of Hurricane Lili on the distribution of organic matter along the inner Louisiana Shelf (Gulf of Mexico, USA). Cont. Shelf Res 26, 2260-2280.

Keller, G., Bentley, S.J., Xu, K., Maloney, J., Miner, M., Georgiou, I., 2016, River-plume sedimentation and 210Pb/7Be seabed delivery on the Mississippi River delta front. Geo Marine Letters doi:10.1007/s00367-016-0476-0.

Kennedy, Andrew B., et al. "Hurricane Response of Nearshore Borrow Pits from Airborne Bathymetric Lidar." *Journal of Waterway, Port, Coastal, and Ocean Engineering*, vol. 136, no. 1, 2010, pp. 46–58., doi:10.1061/(asce)ww.1943-5460.0000024.

Khalil, S.M., Finkl, C.W., Andrews, J. and Knotts, C.P., 2007. Restoration-quality sand from Ship Shoal, Louisiana: geotechnical investigation for sand on a drowned barrier island. In Coastal Sediments' 07 (pp. 685-698).

Kindinger, J., Flocks, J., Kulp, M., Penland, S., Britsch, L.D., Brewer, G., Brooks, G.L., Dadisman, S., Dreher, C. and Ferina, N., 2001. Sand resources, regional geology, and coastal processes for the restoration of the Barataria barrier shoreline (No. 2001-384).

Knutson, T. R., J. L. McBride, J. Chan, K. Emanuel, G. Holland, C. Landsea, I. Held, J. P. Kossin, A. K. Srivastava, and M. Sugi (2010), Tropical cyclones and climate change, Nat. Geosci., 3, 157–163, doi:10.1038/ngeo779.

Kulp, M., Penland, S., Williams, S.J., Jenkins, C., Flocks, J. and Kindinger, J., 2005. Geologic framework, evolution, and sediment resources for restoration of the Louisiana coastal zone. Journal of coastal research, pp.56-71.

Lin, J., Li, C., Boswell, K.M., Kimball, M., Rozas, L., 2016. Examination of winter circulation in a northern Gulf of Mexico estuary. Estuary. Coasts 39, 879–899. https://doi. org/10.1007/s12237-015-0048-y.

Liu, H., Xu, K.H., Li, B., Han, Y., Li, G., 2019 Sediment Identification Using Machine Learning Classifiers in a Mixed-Texture Dredge Pit of Louisiana Shelf for Coastal Restoration. Water, 11, 1257. https://www.mdpi.com/2073-4441/11/6/1257.

Lu, Q., Nairn, R.B., 2011. Prediction on morphological response of dredged sand-borrow pits. Coastal Engineering Proceeding 1 (32), 74.

McBride, Randolph A., and Mark R. Byrnes. "Regional Variations in Shore Response along Barrier Island Systems of the Mississippi River Delta Plain: Historical Change and Future Prediction." *Journal of Coastal Research*, vol. 13, no. 3, 1997, pp. 628–655.

Meade R., 1995. Contaminants in the Mississippi River. U.S. Geo- logical Survey Circular 1133, Reston, VA.

Miller, R.L.; McKee, B.A. Using MODIS Terra 250 m imagery to map concentrations of total suspended matter in coastal waters. Remote Sens. Environ. 2004, 93, 259–266.

Miner, Michael D., et al. "Delta Lobe Degradation and Hurricane Impacts Governing Large-Scale Coastal Behavior, South-Central Louisiana, USA." *Geo-Marine Letters*, vol. 29, no. 6, 2009, pp. 441–453., doi:10.1007/s00367-009-0156-4

Moeller, C.C., Huh, O.K., Roberts, H.H., Gumley, L.E. and Menzel, W.P., 1993. Response of Louisiana coastal environments to a cold front passage. Journal of Coastal Research, pp.434-447.

Mossa, J. and Roberts, H.H., 1990. Synergism of riverine and winter storm-related sediment transport processes in Louisiana's coastal wetlands.

Murray, S.P., 1998. An observational study of the Mississippi-Atchafalaya coastal plume.

Nairn, R., Q. Lu and S. Langendyk 2005. A study to address the issue of seafloor stability and the Impact on Oil and Gas infrastructure in the Gulf of Mexico. US Dept. of the Interior, MMS, Gulf of Mexico OCS Region, New Orleans, LA OCS Study MMS 43: 179.

National Oceanic and Atmospheric Administration (NOAA), 2010. Annual Commercial Landing Statistics. http://www. st.nmfs.noaa.gov/st1/commercial/landings/annual_landings. html.

Obelcz, J., Xu, K., Georgiou, I. Y., Maloney, J., Bentley, S. J., & Miner, M. D. (2017). Sub-decadal submarine landslides are important drivers of deltaic sediment flux: Insights from the Mississippi River Delta Front. *Geology*. doi:10.1130/g38688.1

Obelcz, J., Xu, K., Bentley, S. J., O'Connor, M., & Miner, M. D. (2018). Mud-capped dredge pits: An experiment of opportunity for characterizing cohesive sediment transport and slope stability in the northern Gulf of Mexico. *Elsevier*, 161-169.

O'Connor, M., 2017. Sediment Infilling of Louisiana Continental-shelf Dredge Pits: A Record of Sedimentary Processes in The Northern Gulf of Mexico. M.S. Thesis, Louisiana State University, 68pg.

Olsen, C. R., Larsen, I. L., Lowry, P. D., Cutshall, N. H., & Nichols, M. M. (1986). Geochemistry and deposition of7Be in river-estuarine and coastal waters. *Journal of Geophysical Research*, *91*(C1), 896. doi: 10.1029/jc091ic01p00896

Penland, S., Suter, J. R., & Moslow, T. F. (1986). Inner-shelf shoal sedimentary facies and sequences: Ship Shoal, northern Gulf of Mexico. The Society of Economic Paleotologists and Mineralogists, 73-123.

Penland, S., and Boyd, R., 1981, Shoreline changes on the Louisiana barrier coast: IEEE Oceans, v. 81, p. 209-19

Penland, S., Suter, J.R. and Moslow, T.F., 1986. Inner-shelf shoal sedimentary facies and sequences: Ship Shoal, northern Gulf of Mexico.

Penland, S. and Ramsey, K.E., 1990. Relative sea-level rise in Louisiana and the Gulf of Mexico: 1908-1988. Journal of Coastal Research, pp.323-342.

Restreppo, G.A., Bentley, S.J., Wang, J. and Xu, K., 2019. Riverine Sediment Contribution to Distal Deltaic Wetlands: Fourleague Bay, LA. Estuaries and Coasts, 42(1), pp.55-67.

Roberts, H.H., 1997, Dynamic changes of the Holocene Mississippi River delta plain: the delta cycle: Journal of Coastal Research, p. 605-627

Robichaux, P., Xu, K., Bentley, S. J., Miner, M. D., & Xue, Z. G. (2020). Morphological evolution of a mud-capped dredge pit on the Louisiana shelf: Nonlinear infilling and continuing consolidation. *Geomorphology*, *354*, 107030. doi:10.1016/j.geomorph.2019.107030

Rotondo, K.A., and S.J. Bentley. 2003. Deposition and resuspension of fluid muds on the western Louisiana inner continental shelf. Gulf Coast Association of Geological Societies Transactions 53: 722–731.

Saucier, R.T., 1994, Geomorphology and Quaternary Geologic History of the Lower Mississippi Valley. Volume 2: DTIC Document.

Singh, S., D'Sa, E., and Swensen, E., 2010. Seasonal variability in CDOM absorption and fluorescence properties in the Barataria Basin, Louisiana, USA. Journal of Environmental Science,22(10): 1481-1490.

Stone, G.W., Condrey, R.E., Fleeger, J.W., Khalil, S.M., Kobashi, D., Jose, F., Evers, E., Dubois, S., Liu, B., Arndt, S. and Gelpi, C., 2009. Environmental investigation of long-term use of Ship Shoal sand resources for large scale beach and coastal restoration in Louisiana. US Dept. of the Interior, Minerals Management Service, Gulf of Mexico OCS Region, New Orleans, LA. OCS Study MMS, 24, p.278.

Stone, G. W., Pepper, D.A., Xu, J., and Zhang, X., 2004, Ship shoal as a prospective borrow site for barrier island restoration, coastal south-central Louisiana, USA: Numerical wave modeling and field measurements of hydrodynamics and sediment transport: Journal of Coastal Research, p. 70-88

Syvitski, James P. M., et al. "Sinking Deltas Due to Human Activities." *Nature Geoscience*, vol. 2, no. 10, 2009, pp. 681–686., doi:10.1038/ngeo629.

Twilley, R.R., 2007. Coastal Wetlands and Global Climate Change: Gulf Coast Wetland Sustainability in a Changing Climate. Arlington, Virginia: Pew Center on Global Climate.

Twilley, Robert R., et al. "Co-Evolution of Wetland Landscapes, Flooding, and Human Settlement in the Mississippi River Delta Plain." *Sustainability Science*, vol. 11, no. 4, 2016, pp. 711–731., doi:10.1007/s11625-016-0374-4.

Walker, N.D., 1996. Satellite assessment of Mississippi River plume variability: causes and predictability. *Remote Sensing of Environments*, 58, 21-35

Walker, N.D., and Hammack, A. B., 2000, Impacts of winter storms on circulation and sediment transport: Atchafalaya Vermillion Bay region, Louisiana, USA: Journal of Coastal Research, p. 996-1010.

Walker, N. D., W. J. Wiseman Jr, L. J. Rouse Jr and A. Babin (2005). "Effects of river discharge, wind stress, and slope eddies on circulation and the satellite-observed structure of the Mississippi River plume." Journal of Coastal Research: 1228-1244.

Walsh, J., & Nittrouer, C. (2009). Understanding fine-grained river-sediment dispersal on continental margins. *Marine Geology, 263*(1-4), 34-45.

Wang, J., Li, C., & Obelcz, J. B. (2018). Forces Driving the Morphological Evolution of a Mud-Capped Dredge Pit, Northern Gulf of Mexico. Water, 2018(20), 1001st ser., 1-13.

Wiseman, W.J., JR.; Bane, J.M.; Murray, S.P., and Tubman, M.W., 1976. Small-scale temperature and salinity structure over the inner shelf west of the Mississippi River delta. Memoires Societe Roy- ale des Sciences de Liege. 6e serie. 10, 277–285.

Xue, Z., Wilson, C.A., Xu, K.H., Bentley, S.J., and Liu, H., (*in review).* Sandy Dredge Pit Sedimentation—Characteristics and Processes in Caminada Borrow Area, Ship Shoal, Louisiana Shelf, USA

Xu, K., Mickey, R. C., Chen, Q., Harris, C. K., Hetland, R. D., Hu, K., & Wang, J. (2016). Shelf sediment transport during hurricanes Katrina and Rita. *Computers & Geosciences, 90,* 24-39. doi:10.1016/j.cageo.2015.10.009

Xu, K., Harris, C.K., Hetland, R.D., and Kaihatu, J.M., 2011, Dispersal of Mississippi and Atchafalaya sediment on the Texas-Louisiana shelf: Model estimates for the year 1993: Continental Shelf Research, v. 31, no. 15, p. 1558-1575.

Vita

Matthew Barley was born in Columbus, Indiana and grew up in Terre Haute, Indiana. He received his B.S. in Geology from Indiana State University in 2018. Matthew developed an interest in coastal sedimentology while taking a technical writing class in his junior year of college. This interest led him to work with Dr. Carol Wilson at Louisiana State University in 2018 researching coastal borrow areas in Louisiana. Matthew plans on receiving his Master of Science degree in December 2020.